Linköping University | Department of Biomedical Engineering
Master's thesis, 30 ECTS | Elektroteknik
2023 | LIU-IMT-TFK-A—23/710–SE

Development of a tool for analysis and visualization of longitudinal magnetic resonance flow measurements

– of subarachnoid hemorrhage patients in the neurointensive care unit

---

Utveckling av verktyg för analys och visualisering för longitudinella magnetresonans flödesmätningar

Ildi Adok

Supervisor : Anders Tisell Ph.D, Sofie Tapper Ph.D
Examiner : Professor Karin Wårdell, Tekn. Dr

LINKÖPING UNIVERSITY

Linköpings universitet
SE–581 83 Linköping
+46 13 28 10 00 , www.liu.se

Abstract

Patients who are treated in an intensive care unit need continuous monitoring in order for clinicians to be prepared to intervene should a secondary event occur. For patients treated at the neurointensive care unit (NICU) who have suffered a subarachnoid hemorrhage (SAH) this secondary event could be ischemia, resulting in a lack of blood flow. Blood flow can be measured using magnetic resonance imaging (MRI). The process is facilitated with a software called NOVA. Repeated measurements can therefore be performed as a way to monitor the patients, which in this context would be referred to as longitudinal measurements. As more data can be collected ways of analyzing and visualizing the data in a comprehensible way is needed. The aim of this thesis was therefore to develop and implement a method for analyzing and visualizing the longitudinal MR measurement data. With this aim in mind two research questions were relevant. The first one was how NOVA flow longitudinal measurements can be visualized to simplify interpretation by clinicians and the second one was in what ways the longitudinal data can be analyzed. A graphical user interface (GUI) was created to present the developed analysis and visualization tool. Development of the tool progressed using feedback from supervisors and neurosurgeons. Visualization and analysis was done through plots of blood velocity and blood flow as the main component as well as a 2D vessel map. The final implementation showed multiple examples of how the longitudinal data could be both visualized and analyzed. The results therefore provided a tool to analyze and visualize NOVA flow longitudinal measurements in a way which was easily interpreted. Further improvements of the tool is possible and an area of improvement could involve increasing the adaptability of the tool.

Acknowledgements

To begin with I would like to thank my examiner Karin Wårdell together with my supervisors Anders Tisell and Sofie Tapper for the opportunity to be part of this project. I am grateful for their support, help and multiple insightful and interesting discussions throughout this thesis. I would also like to thank the neurosurgeons at Linköping University Hospital for their time and valuable feedback given during this thesis.

I would also like everyone at the neuroengineering department for creating a positive and welcoming environment during my time with you. A special thanks to my office colleagues Elisabeth and Stina for the continuous inspiring environment as well as to all the discussions arising from interesting questions. Not to forget, I would like to thank all classmates I have had the pleasure of meeting during my years at Linköping University.

A final thank you to my family and especially my parents who have been an important part of my academic journey all these years.

Contents

List of Figures

List of Tables

Notations

Table 0.1: List of used general abbreviations.

Abbreviation	Explanation
ASL	Arterial Spin Labeling
CBF	Cerebral Blood Flow
CBV	Cerebral Blood Flow
CNS	Central Nervous system
CT	Computed tomography
CTP	CT Perfusion
DCE	Dynamic contrast enhanced
DSA	Digital Subtraction Angiography
DSC	Dynamic Susceptibility
GUI	Graphical User Interface
iMRI	intra Operative MRI
MR	Magnetic Resonance
MRI	Magnetic Resonance Imaging
MTT	Mean Transit Time
MFV	Mean Flow Velocity
NICU	Neurointensiva Care Unit
RBC	Red Blood Cell
RF	Radiofrequency
SAH	Subarachnoid Hemorrhage
TCD	Transcranial Doppler
Tmax	Time to maximum
TOF	Time of Flight
TR	Repetition Time
Xe-CT	Xenon CT

List of Vessels

Table 0.2: List of used vessel abbreviations.

Abbreviation	**Explanation**
LICA	Left Internal Carotid Artery
RICA	Right Internal Carotid Artery
BA	Basilar Artery
LMCA	Left Middle Cerebral Artery
RMCA	Right Middle Cerebral Artery
LPCA	Left Posterior Cerebral Artery
RPCA	Right Posterior Cerebral Artery
LACA2	Left Anterior Cerebral Artery
RACA2	Right Anterior Cerebral Artery
LVA	Left Vertebral Artery
RVA	Right Vertebral Artery

1 Introduction

The NICU treats patients suffering from conditions such as traumatic brain injury and SAH. Treatment at the NICU is needed due to the high risk of a secondary ischemic event [1]. Ischemia meaning a lack of or insufficient blood flow to the cells of the body, a cerebral ischemia in this case [2]. Therefore, monitoring physiological parameters, such as the cerebral blood flow (CBF) of the major arteries, is important in order to notice these potentially dangerous events and start preventative treatment in time.

There are many different techniques for measuring CBF, both invasive and non-invasive, as well as more continuous measurements versus snapshot measurements. These techniques include ultrasound doppler, MRI and angiography [3], as well as different variations of computed tomography [4] [5]. The NICU at Linköping University Hospital has a unique setup available with a MRI system located at the NICU department. This setup enables MR based flow measurements of SAH patients treated at the NICU without putting the patient through the risk of medical transportation. NOVA is a software which aids planning and performance of velocity and flow measurements of major vessels in the brain done with the MRI system. This new option of performing repeated MR flow measurements in the NICU is a great advantage for the patients as no radiation is needed, which is not always the case with other monitoring methods. The new method does however generate a need for methods of analysis and visualization of the longitudinal data. These visualizations and analysis methods should be easy to quickly interpret by a clinician. At this time the usage of NOVA flow on SAH patients as well as using NOVA flow for longitudinal measurements has not yet been validated for clinical use.

1.1 Project background

The neuroengineering group at Linköping University Hospital is currently working on a large project named *Multimodal guidance in neurosurgery*. The purpose of this project is to combat neurosurgical disorders such as brain tumors, aneurysm bleedings and brain trauma through implementation of novel biomedical optic systems and unique developed concept of using intraoperative MRI (iMRI). There are multiple objectives in this project regarding the inclusion of optical tools to be used in neurosurgery and neurointensive care. The objective mainly related to this thesis is however the objective of studying, monitoring and imaging

CBF and microcirculation of patients placed in neurointensive care. Detecting events such as secondary bleedings or vasospasm, which could lead to further complications, at an early stage would be considered a success in the project context.

The possibility to measure CBF for multiple larger vessels of the brain with MRI and NOVA over multiple days at the NICU at Linköping University Hospital generates an increased amount of data. Data which is more useful if presented in a way that is comprehensible for the personnel involved. Thereby this thesis becomes part of the process of striving for useful analysis and visualization tools to contribute to the continued progress of the described project.

1.2 Aim

The aim of this thesis was to develop and implement a method for analyzing and visualizing the longitudinal NOVA flow results, which can be useful for SAH patients. The suggested method was evaluated on real data sets. Software to read the longitudinal data was implemented and a graphical user interface (GUI) was developed for the purpose of analysis and visualization of data. A special interest was directed towards making the GUI user friendly and the results easily interpretable by clinicians working in the NICU.

1.3 Research questions

1. How can NOVA flow longitudinal measurements be visualized to simplify interpretation by clinicians?
2. What are possible ways of analyzing NOVA flow longitudinal measurements?

1.4 Thesis outline

The thesis contains the theory necessary to understand the connection between the measured data and the results, described in chapter 2. The theory contains both a more physiological aspect, where SAH and blood flow is the main focus, and a more technical aspect where the MR flow techniques are described. Chapter 2 also includes descriptions of alternative methods to study blood flow. The methodology of this thesis is described in chapter 3. The results, including the implemented graphical user interface, are presented in chapter 4. Lastly the discussion as well as conclusions drawn from this thesis are found in chapters 5 and 6.

2 Theory

In this chapter, an anatomical and theoretical background necessary for the thesis is presented. From the anatomical perspective, general brain anatomy and more details about SAH are included. General theory about flow is described as well. To understand the used software NOVA, a background of MRI is described. Alternative methods to study blood flow are pesented.

2.1 Anatomy of the brain

The brain is an organ with great complexity capable of many things and controls of vital functions such as breathing and motor skills. The central nervous system (CNS) is made up of the brain along with the spinal cord. There are multiple ways to look at the brain through different divisions. One way is to consider the brain as grey matter and white matter. Grey matter would be the outer portion of the brain while white matter the inner portion, which can be seen to the left of figure 2.1. The main components of white and grey matter are made up of parts of neurons, or in other word nerve cells. Neurons general components are a cell body (soma) and a long stem (axon) as seen in the middle of figure 2.1. The axon can in turn be covered with protective coating called myelin. Grey matter is mostly made up from the somas while for white matter it is the axons. Thus the brain contains a lot of neurons responsible for many important functions of the human body [6].

Another way of dividing the brain is into the cerebrum, cerebellum and brainstem as seen to the right in figure 2.1. The cerebrum contains the grey and white matter, the brainstem acts as a connection between the cerebrum and spinal cord and finally the cerebellum is located at the back of the brain. The cerebral cortex as it is called, is a term which describes the outer grey matter which covers the cerebrum. Between the skull and the brain tissue there are three membrane layers called meninges which have a protecting purpose. Dura mater is the layer closest to the skull, followed by the arachnoid and lastly the innermost layer is called the pia mater, as seen in figure 2.2 [6].

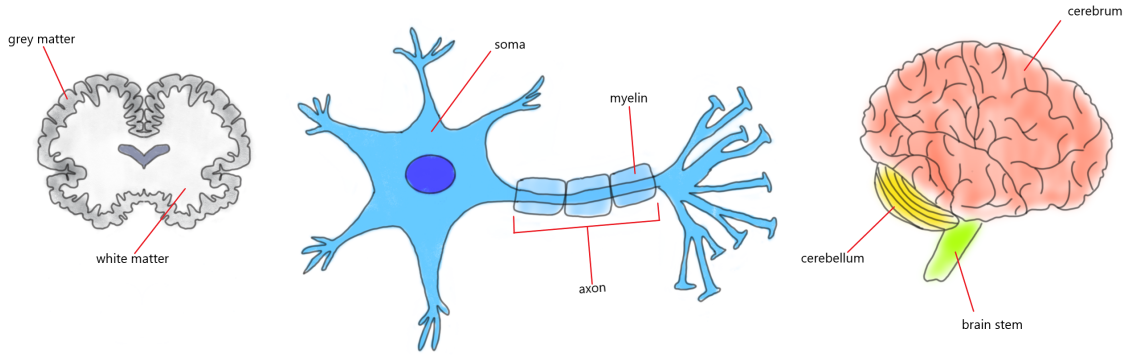

Figure 2.1: Left: White and grey matter. Middle: A neuron. Right: Brain division at a high level.

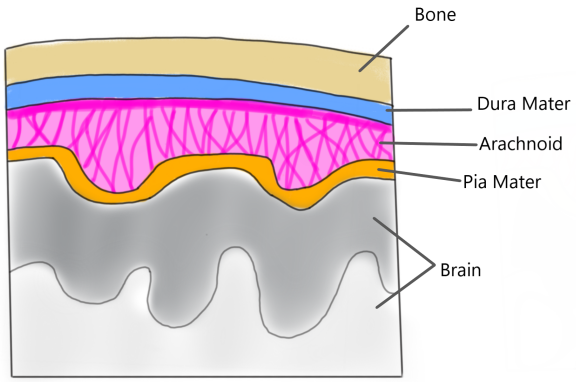

Figure 2.2: The different layers, meninges, protecting the brain.

2.2 Cerebral circulation and blood supply of the brain

Circulation can be divided into anterior circulation and posterior circulation, supplying different areas of the brain through different vessels. A map of the vessels of the brain is seen in figure 2.3. The brain is supplied with blood from the vertebral arteries (VA) as well as the internal carotid arteries (ICA). The internal carotid arteries in turn divide to form the anterior cerebral arteries (ACA) and the middle cerebral arteries (MCA), which form the anterior circulation supplying the forebrain. The forebrain includes the cerebrum. The basilar artery (BA) is formed as the vertebral arteries come together. The blood supply from the basilar artery and the internal carotid arteries are joined and form part of the so-called circle of Willis, which works as a connection between the anterior and posterior cerebral circulation. Emerging from the confluence that is the circle of Willis are the posterior cerebral arteries (PCA) as well as the anterior communicating arteries (ACOM) and the posterior communicating arteries (PCOM). The posterior circulation is made up of PCA, BA and VA and supplies the posterior cortex as well as the brainstem [7]. LACA2 and RACA2, as seen in figure 2.3, are defined as the continuation of LACA and RACA placed after the anterior communication artery.

Oxygen deprivation is a bigger issue for neurons, which have a high metabolic rate, compared to cells with lower metabolic rates. Oxygen and glucose deprivation is a consequence of insufficient blood supply, possibly causing both transient and even permanent damage to

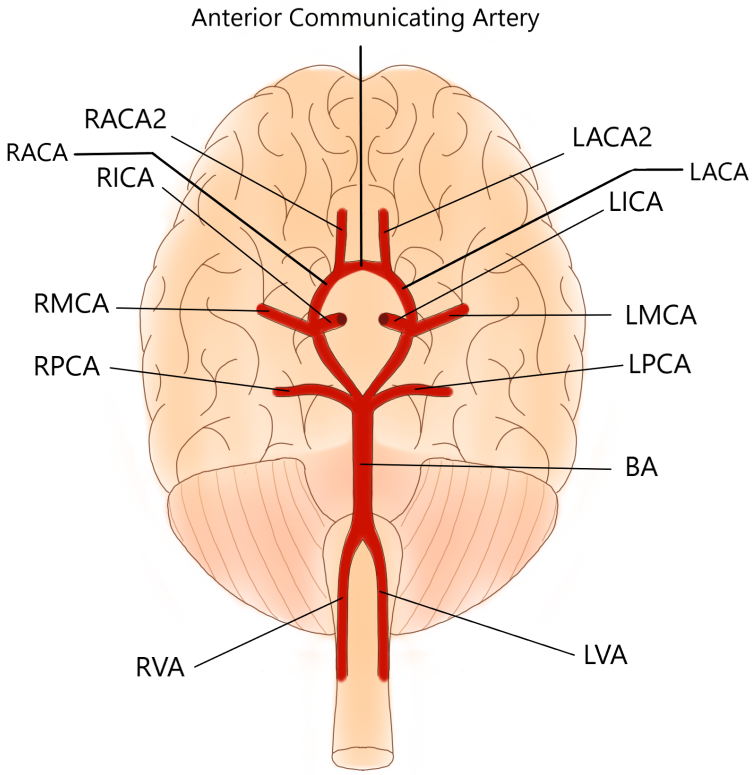

Figure 2.3: Map of the major vessels used in this thesis.

the brain tissue as an outcome. If not treated quickly, cellular changes due to insufficient blood supply (ischemia) could result in cell death [7].

2.3 Subarachnoid Hemorrhage (SAH)

When bleeding occurs in the subarachnoid space, which is beneath the arachnoid, it is called a subarachnoid hemorrhage (SAH). SAH is conisered a medical emergency and immediate treatment and monitoring is necessary [8].

2.3.1 Cause of SAH

Head trauma is one possible cause for of SAH but it may also be the consequence of a ruptured cerebral aneurysm [8]. An aneurysm is a bulge present in a blood vessel due to weakness in the vessel wall. The bulge is the result of pressure caused by blood passing through the weakened area and thus causing the area to expand outwards. Bleeding around the brain would be the consequence if such a bulge eventually ruptures. The majority of SAH events are caused by such a rupture. Risk factors for developing cerebral aneurysms include for instance high blood pressure, smoking, severe head injury and a family history of the same condition [9].

2.3.2 Detection and treatment

A sudden, painful and intense headache is considered one of the main symptoms of SAH. Other symptoms include nausea, vomiting and seizures. Increased intracranial pressure is not uncommon following an SAH [8]. Hyperemia, referring to increased blood flow, following a hemorrhage is one reason the intracranial pressure increases [10]. If the increased

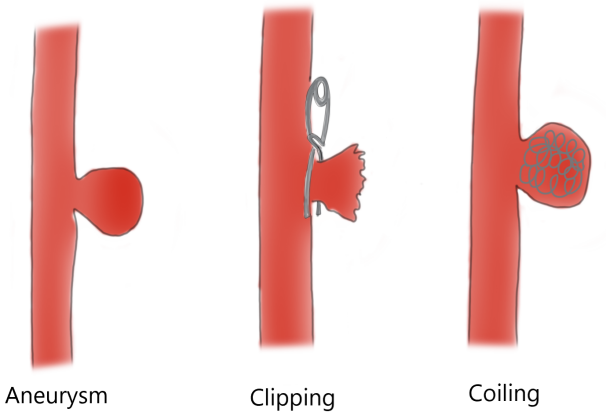

Figure 2.4: Left: An aneurysm. Middle: Clipping of a ruptured aneurysm. Right: Coiling of an aneurysm.

pressure is left untreated, the outcome is in worst case fatal [11].

When suspecting a SAH, a computerized tomography (CT) scan is performed on the patient's brain in order for the health care providers to actually see the SAH. If the CT scan does not provide sufficient information, given that SAH was suspected, further actions are taken. These actions might include lumbar puncture, which tests the cerebrospinal fluid (CSF) for indication of SAH, or magnetic resonance imaging (MRI), which might find bleeding in the brain considered subacute [1].

Treatment for SAH could require being placed in an neurological intensive care unit (NICU). The purpose of treating SAH is to save the patient's life but also to repair the source of bleeding, relieve symptoms and even prevent complications that might follow. If the cause of the SAH is the result of an injury, surgery might be required to relieve the added pressure by the excess blood and also removing large accumulations of blood. If the SAH is the result of an aneurysm rupturing then surgery would be used to repair said aneurysm [1]. Other than repairing the ruptured vessel, prevention of the aneurysm bursting a second could be necessary. Coiling and clipping are two techniques used for this purpose. Coiling is based on the principle of filling the aneurysm with tiny coils obstructing blood from entering and thus preventing the aneurysm's growth and potential rupture again. Clipping is based on clipping the aneurysm at its base in order to seal it. The blood vessel would then heal over time and thereby permanently seal the clipped aneurysm, preventing growth and a second rupture [12]. In figure 2.4 an aneurysm, clipping and coiling are seen.

2.3.3 Complications post SAH

One possible complication following a SAH is vasospasm, resulting from arterial smooth muscle being contracted during a sustained period of time and thus narrowing the subarachnoid arteries. The consequences of vasospasm, one example being infarction, may cause disabilities or even death. Three to five days after the SAH occurs, vasospams begins. Maximal narrowing is found at six to eight days [13]. Delayed cerebral ischemia (DCI) is another example of event which might occur after the SAH. It is essentially insufficient blood supply to the affected area of the brain, and might lead to an increased risk of death [14].

2.4 Blood flow

Fluids in general can be characterized in many ways. Viscous fluid can have laminar or turbulent flows, where flow with a smooth transition characterize laminar regions and time-dependent fluctuations of the fluid properties characterize turbulent regions. These fluid properties include for example viscosity, acceleration and velocity. A simplified way to describe blood flow, Q, is through the relation between the pressure difference across the vessel, ΔP, and the resistance present trying to flow through the vessel, R. This relation is seen in equation 2.1.

$$Q = \frac{\Delta P}{R} \tag{2.1}$$

As multiple properties affect Q and R, equation 2.1 has assumptions made to simplify the relation, such as no temporal variation of the fluid properties. The pressure in this context is meant as the driving force for flow rather than a static pressure difference found across the tissue. Pressure is easier to measure than resistance to flow, which cannot be measured. The resistance can still be calculated from equation 2.1 [15].

Another way to approximate volumetric flow rate, Q, is using Hagen-Poiseuille's law. The approximation is described in equation 2.2.

$$Q = \frac{\pi \Delta P r^4}{8 \mu L} \tag{2.2}$$

The quotient $\Delta P / L$ describes the pressure gradient across a tube which is defined with length L and radius r. Some assumptions made for this approximation include constant viscosity, μ, for the fluid within the tube and fluid parameters which do not vary with time. An equation to calculate the resistance, R, can be derived by combining equation 2.1 and 2.2. The final equation is seen in equation 2.3.

$$R = \frac{8 \mu L}{\pi r^4} \tag{2.3}$$

Given equations 2.2 and 2.3 it can be seen that the resistance is altered significantly even when the vessel radius has small changes. The flow rate will thus experience large changes as well as a consequence of the radius of the vessel changing [15].

A dimensionless parameter called the Reynolds number is defined as in equation 2.4. The parameters included in the equation are fluid density ρ, average fluid velocity across the pipe's cross section V, pipe diameter D and fluid viscosity μ. The Reynolds number is used as a prediction of the transition between the laminar flows and the turbulent flows.

$$Re = \frac{\rho V D}{\mu} \tag{2.4}$$

Since conservation of mass applies given a specific volume, it is known that the mass entering the given volume in a specific time will be the same as the sum of the mass leaving the same given volume over the same time interval. A continuity equation can be defined as given in equation 2.5.

$$\rho_1 A_1 V_1 = \rho_2 A_2 V_2 = constant \tag{2.5}$$

ρ_1 represents the fluid density at point 1, A_1 represents the area in which the studied fluid enters the given area and V_1 represents an average velocity across the area A_1. ρ_2, A_2 and V_2 represent the previously mentioned parameter's counterparts at point 2. Equation 2.5 can be simplified to equation 2.6 when the density of the fluid is considered constant ($\rho_1 = \rho_2$), which is the case for incompressible fluids when the circumstances are that the given volume

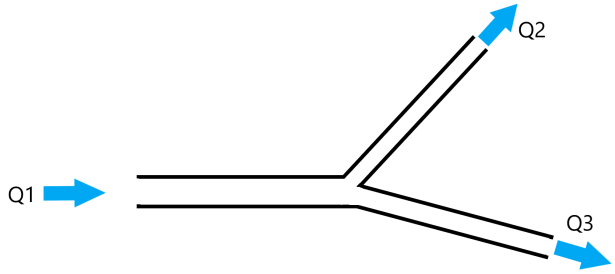

Figure 2.5: Example of branching of a vessel and its corresponding flows.

does not change. Q in equation 2.6 refers to the volume flow rate which goes into and out of the given volume.

$$A_1V_1 = A_2V_2 = Q = constant \tag{2.6}$$

An example of what equation 2.6 implies is given by equation 2.7 where flow at a branching point in an artery is represented [16]. The example is visualized in figure 2.5.

$$Q_1 = Q_2 + Q_3 \; or \; A_1V_1 = A_2V_2 + A_3V_3 \tag{2.7}$$

2.5 Magnetic Resonance Imaging (MRI)

MRI is an imaging technique utilizing certain properties of hydrogen nuclei along with strong magnetic fields and radiofrequency (RF) pulses to generate images. MRI is advantageous mainly due to not requiring radiation to obtain the images. Other advantages include the possibility to generate images in any plane, both two-dimensional and three-dimensional, as well having great contrast for soft tissue. MRI can also be used to measure blood flow. However, MRI requires a longer image acquisition time compared to for instance CT or ultrasound [3].

2.5.1 What is Magnetic Resonance Imaging

There are three major hardware components in the MRI system, each generating a magnetic field with a certain purpose. The first one is the superconducting magnet, creating a strong static magnetic field, with a typical strength of 1.5 or 3 Tesla, which previously was referred to as B_0. Then there are three magnetic field gradient coils which enable the protons precession frequency, sometimes also referred to as resonance frequency, to be spatially dependent of the protons position in the body. Finally the radiofrequency (RF) transmitter and receiver to achieve the induced signal that can be measured and transformed to an image [3].

In the human body there is an abundance of hydrogen atoms, found in for instance water, and the hydrogen nuclei is especially relevant to study for MRI. The hydrogen nuclei consist of a single proton, which is positively charged [17]. Protons have a property called spin, a representation of intrinsic angular momentum, P, with a quantized value. The quantized value for protons is $1/2$ [18]. A magnetic moment, μ, is an intrinsic property of particles with spin $1/2$, which allows the proton to be thought of as a small bar magnet. This property means that when no strong external magnetic field is present, the magnetic moments are oriented randomly, as is seen to the left of figure 2.6 [3]. However, when the protons are placed in a strong magnetic field, B_0, they try to align with the direction of B_0 but will not fully do so. The right side of figure 2.6 visualizes how the protons behave differently when the magnetic field B_0 is present compared to when no magnetic field is present, as seen to the

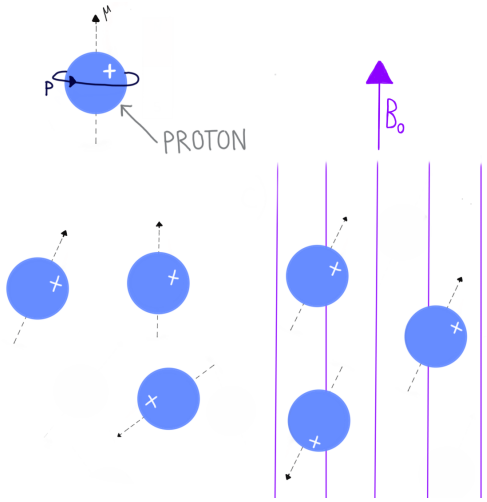

Figure 2.6: Left side showing protons without the presence of an external magnetic field, right side showing protons aligning at .

left in figure 2.6. Particles with spin 1/2 also possess the intrinsic property of precessing. This precession will occur at a frequency which is proportional to B_0. The relationship between the precession frequency ω_0 , or Larmor frequency as it is also called, and B_0 is seen in the Larmor equation presented in equation 2.8 [17].

$$\omega_0 = \gamma B_0 \tag{2.8}$$

Part of the Larmor equation is a constant named the gyromagnetic ratio, γ, which has a certain value for protons [3].

A net magnetization, based on the sum of each proton's individual magnetization component, can be visualized using a vector. In a coordinate system where the z-direction is defined to be in the direction of B_0, the initial net magnetization will only have a value for the z-component, seen in figure 2.7, as the x- and y-components of the vector will cancel each other out. When an RF pulse is applied it will affect the net magnetization. The magnetic moment of the RF pulse is named the B_1 field and has direction which is perpendicular to B_0. Until the RF pulse is turned off, the net magnetization vector will rotate in a direction which is towards the xy-plane. As the RF pulse has been turned off the magnetization will precess at the Larmor frequency ω_0 around the z-axis. A voltage is induced as a consequence of the magnetization oscillating in the xy-plane. Since the magnetization does not preccess in the z-direction, the z-component of the magnetization will not contribute to the signal as no voltage is induced. To measure the MR signal, which is the result of induction, RF coils are used which are sensitive to the magnetization perpendicular to the main magnetic field B_0 [3]. As the RF pulse is turned off the protons, and thereby the net magnetization, will relax back to their equilibrium position which is aligned with the z-axis [17]. The longitudinal relaxation that occurs as the z-component, M_z, recovers to its original state is also referred to as T_1 relaxation [18]. The RF pulse also affects spins by bringing them into so called phase coherence, meaning that all spins point towards the same position on the circle they precess around [17]. T_2 relaxation would be the corresponding transverse relaxation occurring for the xy-component, M_{xy}, as the magnetization decays due to the protons dephasing in the xy-plane [18]. Repeated sequences of gradient and RF pulses are used with a specific repetition time (TR) [17].

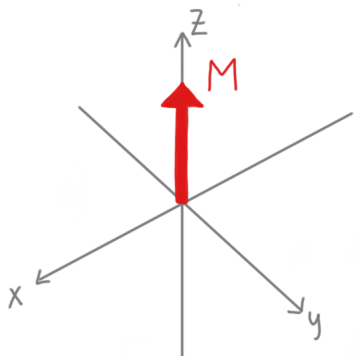

Figure 2.7: Vector representation of net magnetization $\boldsymbol{M}$.

2.5.2 Magnetic Resonance Imaging to measure blood flow

One of the main techniques to achieve contrast between blood vessels and their surrounding tissue using MRI is through the technique called Time of flight (TOF). The technique is based on the difference between how stationary tissue and flowing blood reacts to the multiple repetitive RF pulses applied. The stationary tissue will experience magnetic saturation as a consequence of the RF pulses. Blood that flows into the imaging area will on the other hand have a high initial magnetization due to not having experienced the same RF pulses. The result will be a high contrast between blood and the stationary tissue [18]. An example of a TOF image can be seen in figure 2.8.

A technique used to measure the blood flow is called 2D phase-contrast MRI. Measuring changes in the phase of blood's transverse magnetization is the main principle of phase-contrast imaging. Bipolar gradients are applied and consist of a pair of gradients, which are equal in regard to magnitude but have opposite direction. This type of gradient results in a zero net phase shift for spins that are stationary while moving spins, such as in moving blood, will have a non-zero net phase shift [17]. The phase shift for the moving spins is proportional to its velocity and if spins are flowing in opposite directions but with the same speed this will result in equal but opposite phase shifts. The velocity is thereby computed using the measurements of phase shifts. How sensitive the phase contrast technique is to fast versus slow flows depends on the setting of the bipolar gradients. These settings include amplitude, duration and finally the spacing of the gradients [19]. Additional bipolar gradients are needed to create a known relationship between the blood and the MR signal's phase [17]. As 2D phase contrast MRI measures velocity direction orthogonal to the 2D image slice, a method called 4D flow MRI takes it one step further. 4D flow MRI is a time-resolved 3D phase contrast MRI with flow velocity encoding in three dimensions. Full volumetric coverage can thus be achieved throughout the cardiac cycle due to the 3D measurements of blood flow dynamics [20]. Compared to 2D phase contrast MRI, 4D flow can scan the entire brain with a single acquisition [21]. There exists a trade-off between the whole-brain coverage aspect and a temporal resolution with higher signal to noise ratio levels. 4D flow MRI might therefore require some post-processing to handle the signal to noise ratio [22].

Perfusion describes the delivery of blood to tissue [23]. Magnetic resonance (MR) perfusion imaging is a non-invasive technique where cerebral perfusion is studied by assessing hemodynamic measurements including cerebral blood volume (CBV), CBF and mean transit time (MTT). The volume of blood present in a region of brain tissue is described by CBV, while CBF describes the volume of blood per unit time which passes through a certain region of brain tissue. In this context MTT describes the average time blood takes to pass through a

specific brain tissue region [24]. One type of MR perfusion imaging is arterial spin labeling (ASL). With ASL, quantitative images of the brain perfusion is obtained without needing to administer a contrast agent. Instead, ASL inverts the magnetization of the blood supposed to enter the studied organ, in this case the brain, by applying a train of RF pulses. This blood will reduce the available magnetization in the entered tissue resulting in slightly darker images which then can be subtracted from control images. The amount of blood which has entered the brain since the start of the labeling period can thus be calculated due to the subtracted images being roughly proportional to perfusion rate [25].

Contrast based MR perfusion imaging include dynamic susceptibility contrast-enhanced (DSC) MR perfusion and dynamic contrast-enhanced (DCE) MR Perfusion. For DSC, a gadolinium-based contrast agent is administered and monitored using T2-weighted images. The contrast agent, with paramagnetic properties, has a susceptibility effect which results in a signal loss seen in the intensity-time curve. A contrast medium concentration-time curve can be generated given the signal information, allowing maps of CBV and CBF to be derived. DCE uses T1-weighted images taken before, during and after the contrast agent is administered. The contrast agent could be gadolinium-based too. The generated signal intensity-time curve will provide information about for instance tissue perfusion and vessel permeability. The advantage of DSC and DCE over ASL is a higher signal to noise ratio. An advantage of ASL over DSC and DCE is however not requiring administration of a contrast agent [23].

2.5.3 NOVA FLOW

NOVA (VasSol Inc., Tampa, USA), or Non-invasive Optimal Vessel Analysis, is a software which together with an MRI system provides flow analysis in order to quantify blood flow of vessels in the brain [26]. TOF imaging is used to get a first image in the steps of creating the final 3D vessel model. The image is cropped down to only contain the relevant areas in order to increase efficiency in the steps that follow. An example of how the TOF image looks before and after it has been cropped is seen in figures 2.8 and 2.9. The final 3D model is obtained as the cropped TOF image is segmented and it is now possible, for a trained operator, to mark the measurement points for each vessel that is to be measured. When the measurement point has been marked, NOVA places a plane in the position that is perpendicular to the vessel. The blood flow measurement will thereby be performed on the area that plane covers. The 3D model along with a marked plane on a vessel is seen in figure 2.10.

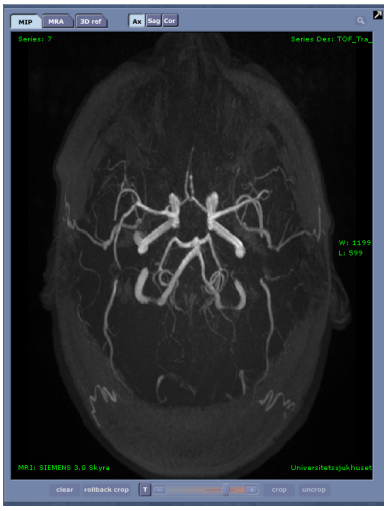

Figure 2.8: Original TOF image from NOVA.

Figure 2.9: Cropped TOF image from NOVA.

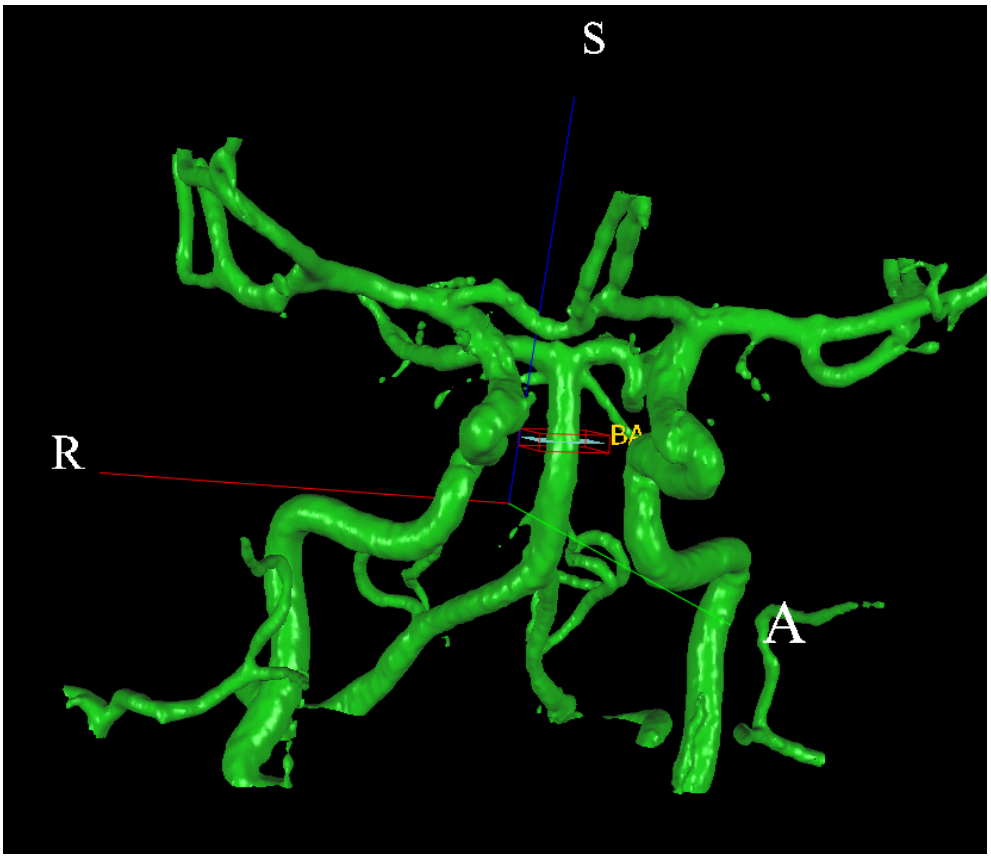

Figure 2.10: Final model which has been segmented. BA plane is marked.

As all measurement planes have been set on the relevant vessels, the 2D phase contrast MRI can proceed. In the resulting image NOVA will automatically mark the area perceived to be the vessel and some manual adjusting to that area may be needed to get the correct area, which should be included in the final presented result. The measured area can be visualized using phase or magnitude representations as seen in an example in figure 2.11. In figure 2.12, the view where all twelve measurements during a cardiac cycle is seen where adjustments can be performed to apply to all measurements or individual cases. Once all the necessary adjustments are done, the resulting blood flow measurements can be saved. If for some reason the measurement was not executed as expected new measurements for the affected vessel or vessels have to be made if possible. An unexpected result for a measurement which would require a new measurement could for instance be the plane supposed to line up perpendicular to the vessel ending up at an incorrect angle, thus affecting the resulting values.

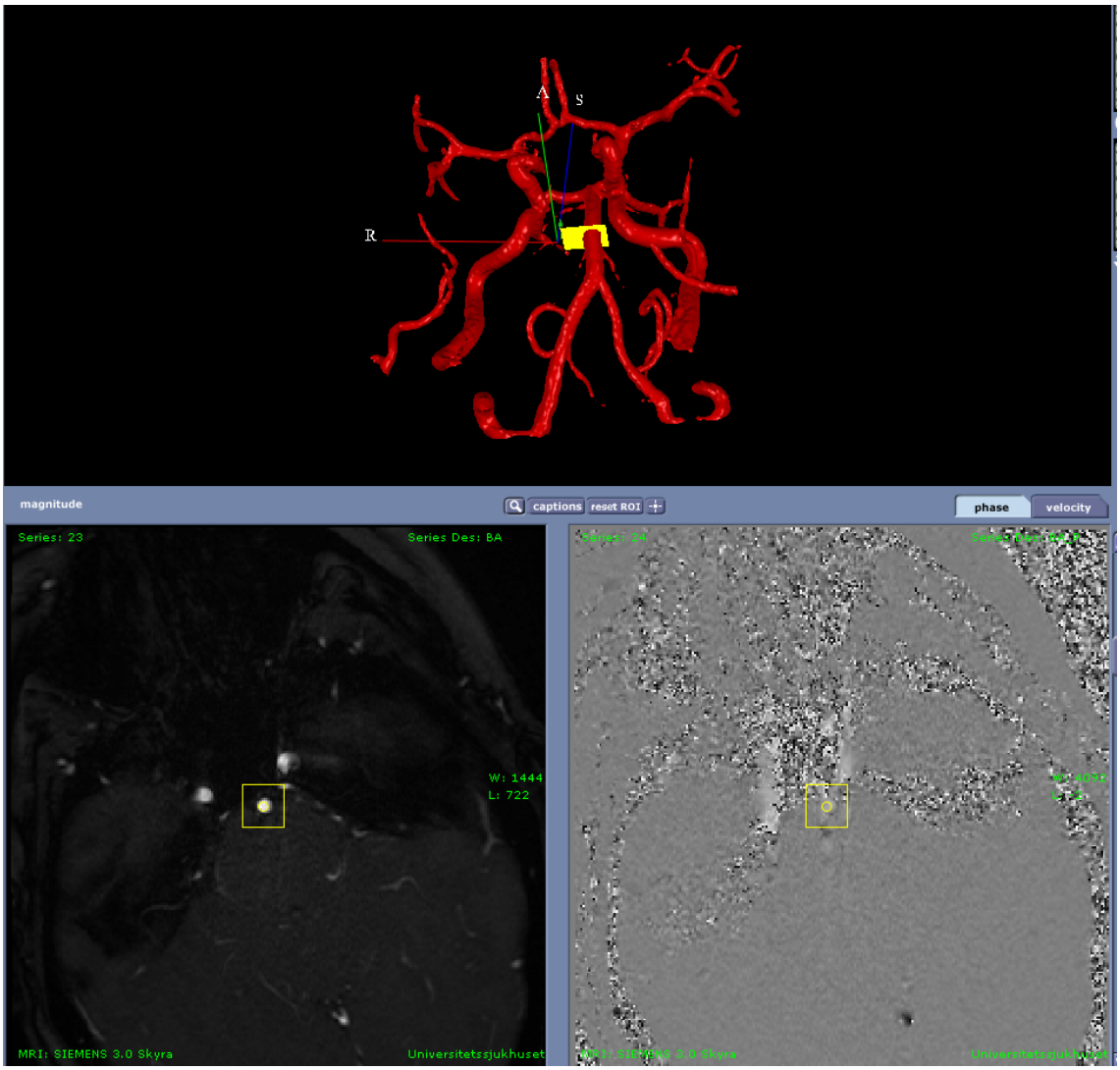

Figure 2.11: View after 2D phase contrast MRI, where phase and magnitude representations of the vessel are seen.

2.6 Alternative methods to study blood flow and blood velocity

Other than MRI, there are other methods and techniques to monitor the CBF, both non-invasive and invasive. Examples of such methods and techniques will be described in the following subchapters.

2.6.1 Ultrasound Doppler

Ultrasound is another medical imaging technique which also can be used to measure blood flow. Ultrasound is essentially a mechanical wave which is produced by a transducer and then transmitted into the tissue being examined. Fractions of energy will be reflected as the wave passes through the tissue and encounters boundaries of tissue possessing different properties, both acoustical and physical. The remaining wave which is not reflected will continue through the tissue until another boundary is encountered and the process part of the wave being reflected and part continuing through will proceed. The reflected wave will travel back to the transducer where it can be detected as a signal. Using the time it took for the wave to be transmitted and to being received, the distance to the boundary where the

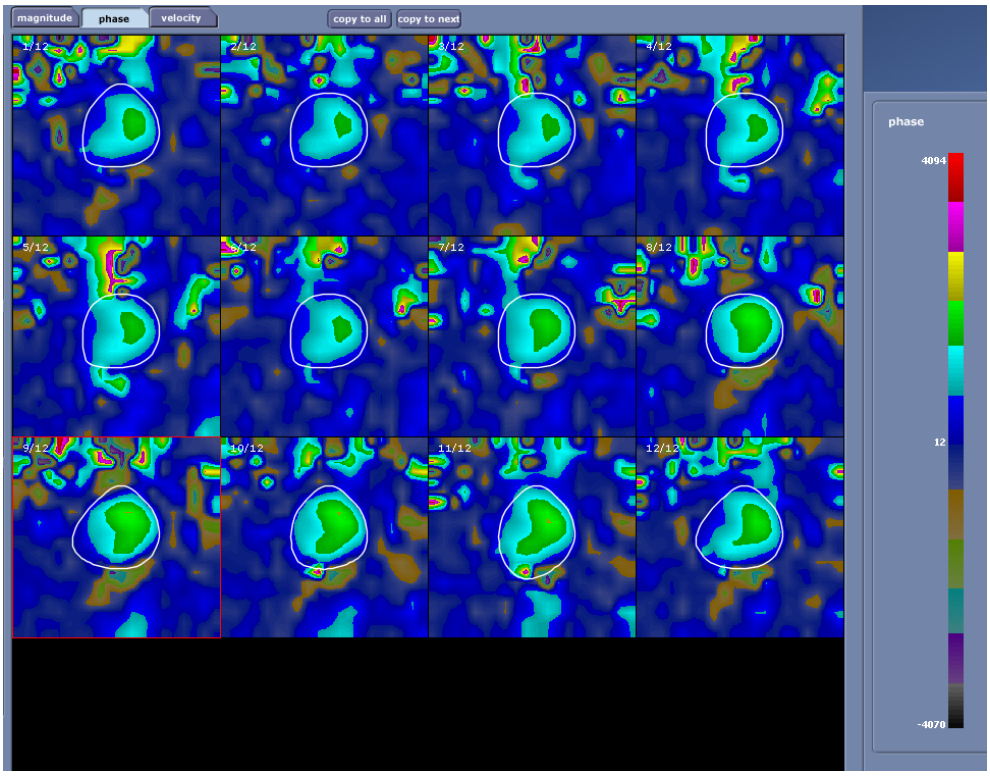

Figure 2.12: View to visualize phase representation of all twelve measurements for a vessel and any adjustment made to the vessel area.

reflection occurred can be calculated [3].

When measuring blood flow with ultrasound, the Doppler effect is taken advantage of. As the ultrasound signal scatters from red blood cells (RBCs) the frequency which the transducer primarily transmitted will be altered as it returns to be detected. The backscattered signal will be at a higher frequency than before if the blood flows towards the transduecer, while the signal will have a lower frequency than before if the blood flows away from the transducer. Certain transducers can be used to measure vessel size, which in combination of the blood velocity values can be used to calculate blood flow [3].

Transcranial Doppler (TCD) is a non-invasive option to monitor patients who have previosly suffered SAH and are now at risk of secondary events. Daily monitoring with TCD is possible unlike other methods such as conventional angiography and CT angiography. These alternative methods are invasive and require contrast agent administration and moving the patient to the department where the equipment is located. TCD can be performed at bedside and could be useful when diagnosing vasospasm. The Lindegaard ratio is an index used as a guide to aid the distinction between hyperemia and vasospasm. Lindegaards ratio is calculated as the mean flow velocity (MFV) of the MCA divided by the MFV of the ICA as seen in equation 2.9.

$$Lindegaard\ ratio = \frac{MFV\ of\ MCA}{MFV\ of\ ICA} \tag{2.9}$$

Based on the MFV of the MCA combined with the Lindegaard ratio, different interpretations can be made. A Lindegaard ratio of 3 and below along with an MFV of either below 120 cm/s or above 200 cm/s is interpreted as an indication of hyperemia. When the Lindegaard ratio is

3 or above it is interpreted as spasm with varying severity, such as mild or moderate spasm, in combination with hyperemia. At a MFV equal to or above 120 cm/s and a Lindegaard ratio between 3 and 6 the severity of the spasm interpretation increases as the ratio increases. A Lindegaard ratio above 6 and a velocity at least above 120 cm/s indicates a moderate to severe spasm [27]. An increase of velocity of more than 50 cm/s during a 24 hour period could also be used as an indicator of vasospasm development [28]

2.6.2 Angiography

Digital subtraction angiography (DSA) is an X-ray technique providing images of high resolution of the blood vessels in the studied body part. To perform the DSA it is necessary to take an initial image. The next step involves using an iodinated contrast agent, which is injected into the bloodstream of the patient. A second image is then taken and image subtraction of the two images is performed in order to more clearly see the vessels in the image [3]. DSA is an invasive procedure requiring a catheter to be inserted into an artery to administer the contrast agent, meaning risks are involved. The risk of stroke exists as the inserted catheter might cause plaque to break off and then potentially block a smaller vessel in the brain. DSA is usually a procedure done to further investigate a previous test results, which maps indicated abnormalities. The results from the DSA technique are more accurate than the results obtained by the TCD technique [29]. Another type of angiography is CT angiography, which uses the CT scanner along with an injected contrast agent to generate images of blood vessels. CT angiography could be useful when diagnosing and evaluating conditions such as aneurysms, blockages, vessel rupture or tears and so on. One advantage of CT angiography over conventional angiography includes the possibility of fewer complications. However, CT angiography still requires the use of radiation, which is considered to a risk if exposure becomes excessive [30].

2.6.3 Xenon CT

Xenon Enhanced Computed Tomography (Xe-CT) is a method used to study the CBF with the help of stable xenon gas. Xenon gas is inhaled, in a mixture combined with oxygen, by the patient and will act as a contrast agent for the CT imaging. This is possible due to properties of the gas, including being radiodense and lipid-soluble. Initial CT scans are completed before inhalation to be used as a baseline. CT scans are then performed both during and following inhalation. To calculate what the xenon arrival curve looks like for each pixel in every slice multiple sets of scans are needed for each level of the brain. To calculate the value for CBF in each pixel the concentration of xenon present in the expired air is also necessary. The concentration in the expired air can be seen as an indirect measure of what the arterial concentration is. One of the main advantages of the use of xenon gas as a contrast agent is that stable xenon is not radioactive. This means that the radiation exposure necessary to acquire the CT images is the only radiation the patient will experience. Xe-CT can also be repeated after 15 minutes as the xenon gas has been eliminated from the body, allowing for repeated measurements if for instance the patient is in a different state due to drug administration [4]. It is possible to safely perform repeated quantitative measurements of CBF in a NICU setting using the Xe-CT method with xenon-inhalation and a mobile CT-scanner [31]. A bedside setup of Xe-CT has been used at Linköping University Hospital.

2.6.4 CT Perfusion

Computed tomography perfusion (CTP) is a technique which does a functional examination of brain tissue in order to characterise the cerebral perfusion state as well as provide information regarding the current status of the patient's circulation. Repeated scans of the brain are done in order to study the contrast agent's flow throughout the region of interest. An

attenuation-time curve is created as the increase, peak and decrease of the contrast agent's flow is measured. Based on the collected information, perfusion parameters representing different hemodynamic properties of each voxel on a CTP map can be calculated. The hemodynamic parameters that are of importance to study with CTP are CBF, CBV, MTT and time to maximum of the residual function (Tmax). CBF describes the amount of blood which flows in a unit of brain mass during a unit of time. CBV is the fraction of vascularized tissue. MTT describes the average time it takes for the administered contrast to cross the capillary bed. Finally, Tmax describes the delay between the start of the scan to when maximum intensity of the contrast agent is achieved in each voxel. Perfusion maps are generated where thresholding might be necessary to achieve greater consistency and objectivity on the results. Perfusion analysis is useful for quantifying tissue where reperfusion might be necessary and still possible for the tissue with significant hypoperfusion as well as identifying irreversibly infarcted tissue, which is in other words known as ischemic core [5].

3 Methodology

This chapter describes the methodology used to develop a tool for analysis and visualization of longitudinal MR flow data.

3.1 Data and measurements

The main data used to develop a tool for analysis and visualization was collected from a healthy volunteer, with no previous head trauma, over six measurement days. Informed written consent was obtained from the healthy volunteer according to the Declaration of Helsinki. This study was approved by the local ethics committee (Dnr 2012/434-31, 2018-143/32). Details about the volunteer can be found in table 3.1, regarding age, gender and number of measurements available

Table 3.1: Volunteer information and details about measurements.

Volunteer	Age and gender	Number of measurements
K6	35 y/o Female	6

The measurements were not necessarily taken over consecutive days due to availability of the volunteer, trained staff and accessibility to the MR scanner. The collected data however is still considered to be longitudinal in the sense that it represents data, in this case changes in cerebral blood flow (CBF), over an extended period of time. Data collection was made approximately at the same time of day every measurement time, namely in the forenoon. By measuring at approximately the same time each measurement day, the idea was for the volunteer's circumstances and state to be roughly similar. This in order to aim for a comparison where the changes in values is based on changes in blood flow between days rather than if the volunteer's blood flow changes possibly are affected by at what time of the day the measurements are performed. Counting the first measurement as performed in day 1 the following measurements were performed on days 3,5,8,9 and 12.

Data collection was made with the use of a magnetic resonance imaging (MRI) system together with the NOVA software, described in chapter 2.5.3. The MRI system used is located in the NICU at Linköping University Hospital. The MRI system was a 3T Siemens Skyra,

equipped with a 20 channel phased-array head coil, and with associated software *Syngo MR EII*. Following an image scout and an initial TOF the correct head position could be confirmed before proceeding with the NOVA software. How NOVA obtains the blood flow measurements is described in more detail in chapter 2.5.3. NOVA allows for personalized measurements based on the patient's vessel anatomy and simplifies the possibly difficult process of placing the measurement plane at the correct angle in relation to the vessel. The NOVA measurements are taken as part of a standard NICU MRI protocol, meaning that other MRI images were obtained as well but not used in this project. The total image acquisition time of the protocol was about an hour. The acquisition time for each vessel with NOVA is however about 20 seconds, but the manual placement of measurement points as well as any necessary retake of measurement might cause the total time to differ. A total of 11 vessels were measured with NOVA and are listed in table 3.2. All vessel abbreviations, excluding BA, begin with an L or R to represent the left and right side. Further on the vessel abbreviation might be used without the beginning L or R when talked about in a more general sense where the side is insignificant.

Table 3.2: Measured vessels using NOVA.

Abbreviation	Vessel Name
LICA	Left Internal Carotid Artery
RICA	Right Internal Carotid Artery
BA	Basilar Artery
LMCA	Left Middle Cerebral Artery
RMCA	Right Middle Cerebral Artery
LPCA	Left Posterior Cerebral Artery
RPCA	Right Posterior Cerebral Artery
LACA2	Left Anterior Cerebral Artery
RACA2	Right Anterior Cerebral Artery
LVA	Left Vertebral Artery
RVA	Right Vertebral Artery

The used data in this thesis is taken from a generated text file where the NOVA measurement results are stored for the specific patient. An example of what the file looks like is shown in figure 3.1. The relevant information to extract from the file was chosen to be *study date, name of the vessel, mean VFR* (Volumetric Flow Rate), the *vfr* (Volumetric Flow Rate) column, the *mean_vel* (mean velocity) column and the *max_vel* (maximum velocity) column. The numbers listed 1 to 12 to the left of the file setup symbolizes that 12 measurements were made, which extend over an entire cardiac cycle. Just as the measurements for LVA are shown for that specific date, there are the same columns found for each vessel that was measured on each measurement day. The area and diameter data was chosen to be excluded as this would potentially be affected by how an operator would mark the vessel area to a greater extent then the other measurements. *wss*, wall shear stress, was decided to be out of scope for this thesis.

3.2 Analysis

As NOVA has not yet become a main tool for longitudinal measurements, the investigated parameters were mainly the same as those usually investigated using for instance TCD. Because changes in MCA velocity may indicate vasospasm as well as looking at the Lindegaard ratio, described in chapter 2.6.1, these two parameters were included in the development of the analysis method. Two changes were of special interest by the clinicians at Linköping

```
loading ReportObject ...
ReportObject software version: 8.1.1
Vendor: SIEMENS
Patient Name: K6
Patient ID: K6
Study Date/Time: 01/30/2023  10:45:03
Heart Rate: 70
Report Status: APPROVED
Creation Date/Time: 02/03/2023  10:14:55
Approve Date/Time:
# of vessels: 11

------------------------------------------------------------------------
Name of the vessel: LVA
Magnitude series no: 20
Phase series no: 21
Name of 3D: HEAD-NECK
Mean VFR: -217.0918
Mean WSS: -11.884159
Mean diameter: 4.7701344
```

image	time_delay(ms)	vfr(ml/min)	mean_vel(cm/s)	max_vel(cm/s)	min_vel(cm/s)	diameter(mm)	area(mm2)	wss(dynes2/cm2)
1	0.0	-221.6953	-20.12553	-44.4	-20.12553	4.8348613	18.359375	-11.655241
2	74.416664	-204.02347	-18.521278	-41.4	-18.521278	4.8348613	18.359375	-10.726176
3	148.83333	-185.6953	-16.857447	-39.0	-16.857445	4.8348613	18.359375	-9.762604
4	223.25	-165.07033	-15.31087	-36.3	-15.31087	4.7831497	17.96875	-8.962807
5	297.66666	-137.34375	-14.292685	-33.8	-14.292683	4.51572	16.015625	-8.862267
6	372.0833	-131.60158	-13.058141	-32.100002	-13.058141	4.624548	16.796875	-7.9062424
7	446.5	-133.21873	-13.218602	-31.300001	-13.218604	4.624548	16.796875	-8.003397
8	520.9166	-217.40622	-19.736168	-39.8	-19.736168	4.8348613	18.359375	-11.42975
9	595.3333	-334.0078	-30.321276	-56.4	-30.321276	4.8348613	18.359375	-17.559874
10	669.75	-336.8906	-30.582973	-56.4	-30.582977	4.8348613	18.359375	-17.711432
11	744.1666	-294.14066	-26.70213	-54.2	-26.70213	4.8348613	18.359375	-15.463928
12	818.5833	-244.00781	-22.151064	-47.3	-22.151064	4.8348613	18.359375	-12.828283

Figure 3.1: Example of measurement results for the vessel LVA, where the relevant data is marked with red bounding rectangles.

University Hospital to include in the analysis method, namely if the velocity of MCA had exceeded 120 cm/s and if the velocity had increased with 50 cm/s or more since the previous day. Other analysis options were explored using the available data and given the amount of information which could be retrieved from the NOVA software to get a sense of what type of analysis would be relevant. These included looking at the range of values during the cardiac cycle, comparing the latest values with an average of all previous measurements, comparing the latest value with the previous measurement and calculating mean and maximum values over the cardiac cycle. Ways to compare the blood inflow and its components was also explored. Total inflow was defined as the sum of LVA, RVA, LICA and RICA.

3.3 Visualization

A previous idea of how the data could be visualized was provided, as seen in figure 3.4, and became a starting point for how the visualization was later developed. This visualization included 7 of the possible 11 vessels measurements. The data was presented using what one could call a radiological convention, mostly seen in medical images where the left half is shown to the right and vice versa, and adding BA in the middle as it has no left and right counterpart. Blood velocity and blood flow are shown separately. MATLAB version R2022a (MathWorks, Natick, USA) was used to implement the visualizations. Plots were the main tool explored for visualizing the data and the different analysis options. The implemented visualizations are shown in chapter 4.

A meeting with two neurosurgeons from Linköping University Hospital was held early in the project to receive feedback on plots where changes and adjustments had been made to the initially provided plot, figure 3.4. The feedback provided a guideline for in which direction the visualization should progress. The plots from the early state of the project are shown in chapter 4. Based on the feedback from the initial meeting a generic 2D vessel map was designed and created to be used in the final visualization tool. The thought was to provide a quick overview of certain changes without being to complicated to look at in order to

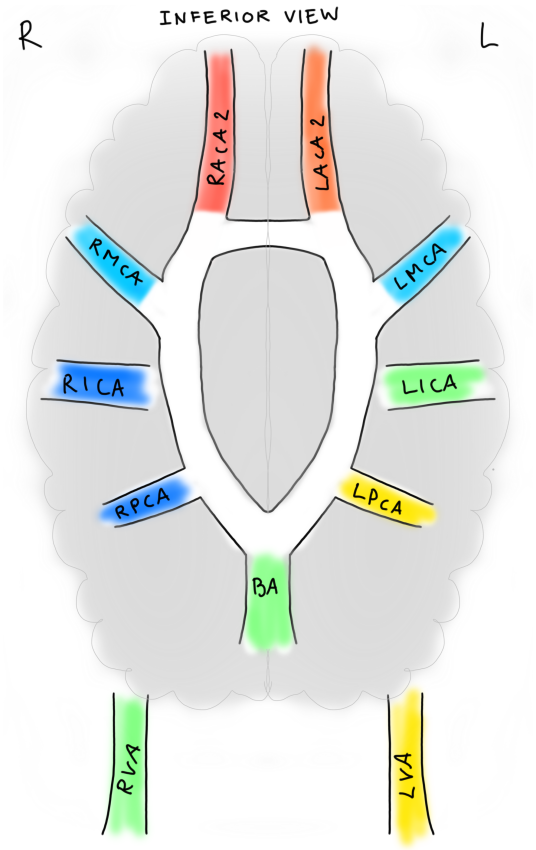

Figure 3.2: First version of the 2D generic vessel map as part of the visualization aspect of the project.

understand the information which is conveyed. A first version of the vessel map is seen in figure 3.2. It shows the concept of visualizing with the help colors and a placement of the vessels in a way that was not too far from reality. Through the development process the vessel map was redesigned and features such as the brain in the background seen in the first version was removed to keep the vessel map simple and without unnecessary distractions. The final version is seen in figure 3.3.

A graphical user interface (GUI) was eventually developed with MATLAB App Designer to be used as the final visualization tool. The resulting GUI and its features are presented in chapter 4. A meeting closer to the end of the project was conducted with the neurosurgeons to receive feedback on the developed GUI. The development process could be thought of including an iterative aspect as the development of the method to analyze and visualize was guided by feedback from the clinicians as well as from the supervisor of this thesis. In order to keep improving the analysis and visualization tool it was necessary to combine feedback and development.

3.4 Verification

Verification of the software's performance was done by inspecting the resulting plots and other components seen in the final GUI based on the input data. Both data which should just be plotted as is and data which has gone through certain calculations before being plotted. As the data was taken from healthy volunteers some cases could not be visualized given

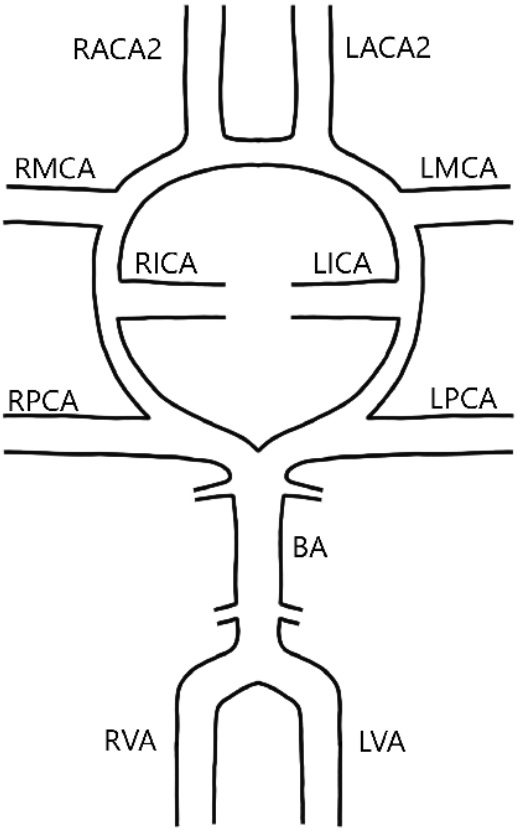

Figure 3.3: Final version of the 2D generic vessel map as part of the visualization aspect of the project.

that the circumstances to be visualized did not happen. This meant that a need to create synthetic data arose. To explore different ideas of what could be visualized given the some of the special cases that could occur in the clinical setting, the volunteer data was modified for certain measurements to achieve the right cases. As the special cases all regarded changes in (maximum) velocity for MCA, as mentioned in chapter 3.2, there was only need to modify the values in the velocity column of the data. Namely the maximum velocity column, as it was eventually decided that the velocity value to be used in the plots in the final tool was the largest value in the maximum velocity column for each measurement day. This meant that the modification could be simplified by change the entire column to the same value, as seen in figure 3.5. The three cases were a velocity value of 120 cm/s or more, an increase of velocity with more than or equal to 50 cm/s since the previous measurement, and the final case would be a combination of the two first cases.

The relevant value to use as velocity representation for each measurement day in the plots in the final tool was data from he maximum velocity column from the data file. The choice was based on limiting how the presented data would be affected by how an operator would mark or adjust the vessel area during the acquisition process. The maximum velocity would thereby be a more consistent measure. As the final tool presents the maximum velocity from the maximum velocity column, the modification of data could be done by setting the same value for all elements in the column. An example of what the modification could look like is seen in figure 3.5.

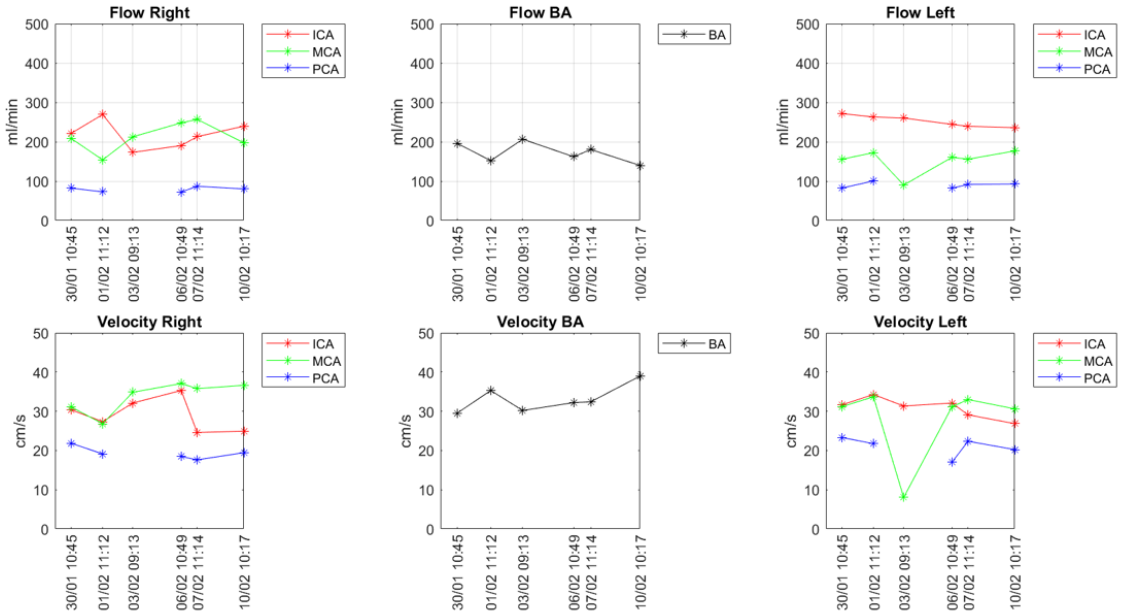

Figure 3.4: Initial visualization idea, including the flow and velocity for BA as well as the left and right equivalents of ICA, MCA and PCA.

```
Name of the vessel: RMCA
Magnitude series no: 13
Phase series no: 14
Name of 3D: HEAD-NECK
Mean VFR: -247.9668
Mean WSS: -27.859827
Mean diameter: 3.7535655
```

image	time_delay(ms)	vfr(ml/min)	mean_vel(cm/s)	max_vel(cm/s)	min_vel(cm/s)	diameter(mm)	area(mm2)	wss(dynes2/cm2)
1	0.0	-194.66014	-30.133331	-115.0	-30.133331	3.7024941	10.766602	-22.788239
2	49.833332	-181.09424	-28.834286	-115.0	-28.834286	3.6507084	10.467529	-22.11516
3	99.666664	-170.3097	-26.363888	-115.0	-26.363888	3.7024941	10.766602	-19.937609
4	149.5	-190.33556	-30.305714	-115.0	-30.305714	3.6507084	10.467529	-23.243708
5	199.33333	-266.2401	-41.213886	-115.0	-41.21389	3.7024941	10.766602	-31.167875
6	249.16666	-321.5804	-47.160522	-115.0	-47.160522	3.803951	11.364746	-34.713764
7	299.0	-343.5443	-46.69512	-115.0	-46.695118	3.951255	12.261963	-33.089825
8	348.8333	-328.5787	-46.95128	-115.0	-46.951283	3.853678	11.663818	-34.113792
9	398.66666	-293.83847	-43.092102	-115.0	-43.092106	3.803951	11.364746	-31.719093
10	448.5	-250.1082	-36.67895	-115.0	-36.678947	3.803951	11.364746	-26.998526
11	498.3333	-221.41516	-35.254284	-115.0	-35.25429	3.6507084	10.467529	-27.039137
12	548.1666	-213.89645	-32.216213	-115.0	-32.21622	3.7535655	11.065674	-24.03192

Figure 3.5: Modified version of data with the purpose to show cases not seen in the healthy volunteer, where the modified column is marked with a box.

4 Results

Plots and visualization options from the early stages of the project are presented in this chapter along with the final GUI and a description of its features.

4.1 Analysis and visualization during early stages of the project

Plots from the early stages of the project are presented in this section. One of the main visualization options explored was a seven in one plot layout, once again inspired by a radiological convention with a left and right side and the BA in the middle. Compared to the initial provided plot, as seen in figure 3.4, the left and right hand side vessels are separated into individual plots. The calculated mean flow is plotted throughout all plots.

Figures 4.1 to 4.5 show variations of the seven plot concept with different alternatives regarding visualization options. In figures 4.1 and 4.2, similar ways of visualizing are used where the difference would lie in color choice of the bars to differentiate the two. Since both flow and mean velocity have twelve values from each date, these plots show two ways of visualizing the range of values during a cardiac cycle. A visual explanation of how the range of values was visualized in figures 4.1 and 4.2 is shown in figure 4.3. The first way to visualize the range of values is done with error bars, where the top and bottom of the error bar represent the maximum and minimum value over the twelve measurements and placed in the plot relative to the mean value of the twelve values. The second way to visualize the range is done by calculating the difference between the maximum and minimum value and then plotting the difference as the height of a bar placed at the bottom of the plot for each measurement date. As can be seen in figure 4.3 the size of the error bars and the colored bar are equal, simplifying a quick comparison between how the range of values differed between measurement days. On the right side of figure 4.1, the error bars are removed to provide an alternative visualization. A way of visualizing if any intervention has been performed before a measurement has taken place is shown in for instance figure 4.2 as a red circle around the date of measurement following the intervention.

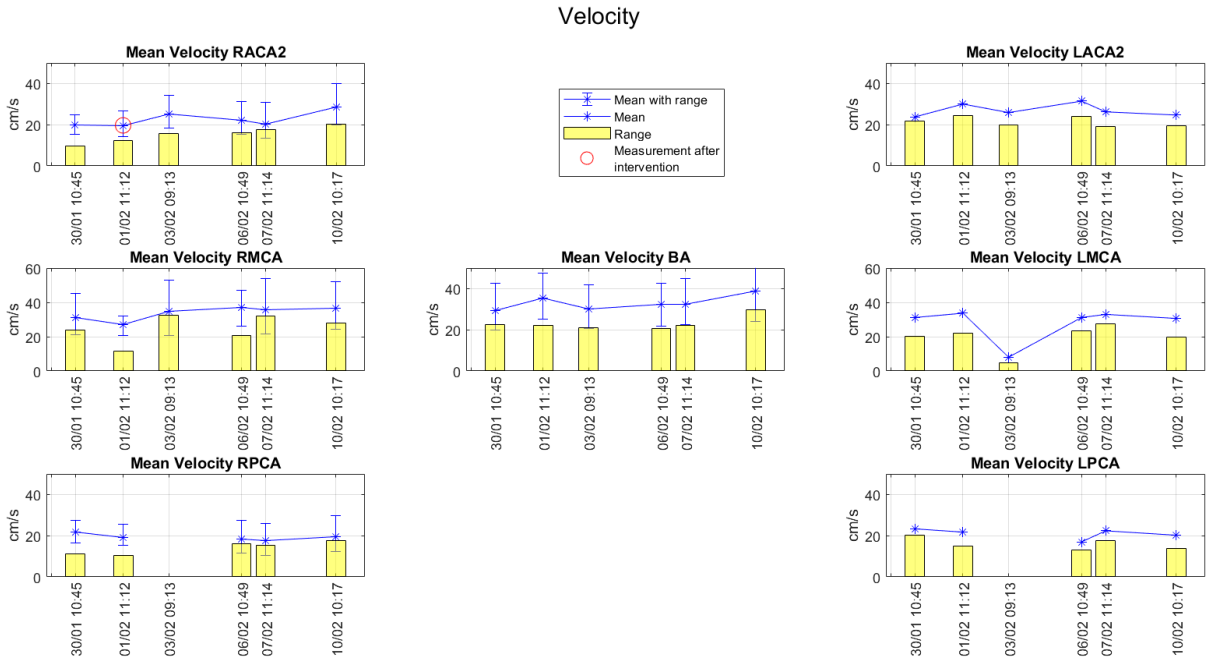

Figure 4.1: Seven plot in one, visualizing mean velocity together with the range of values over a cardiac cycle.

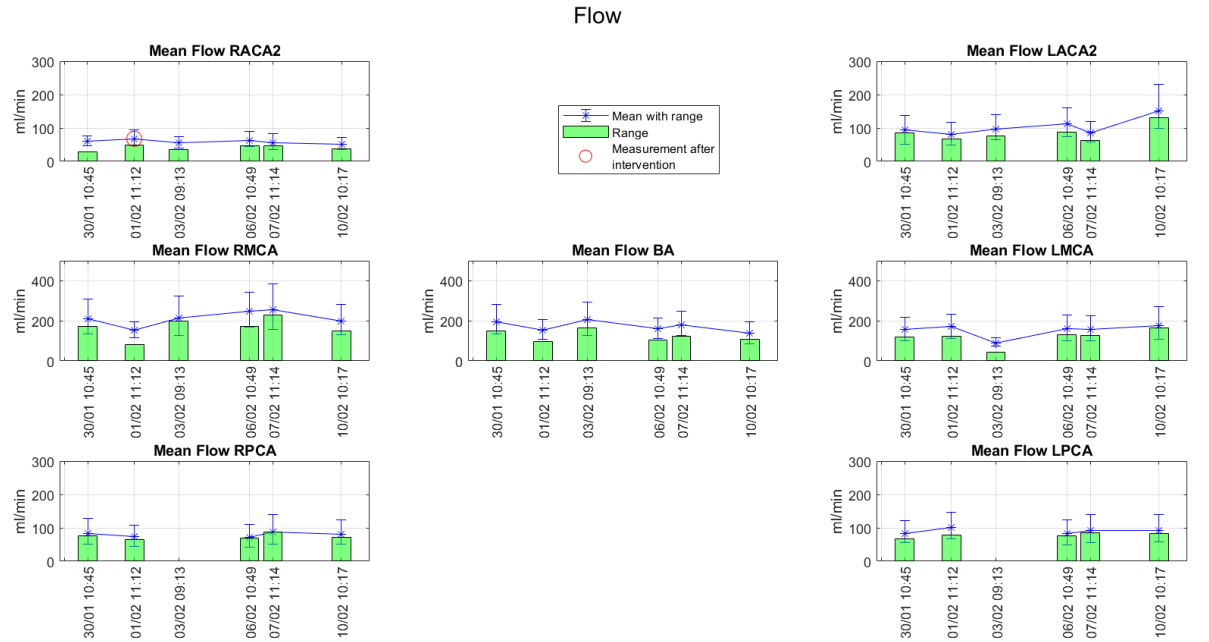

Figure 4.2: Seven plot in one visualizing flow together with the range of values over a cardiac cycle.

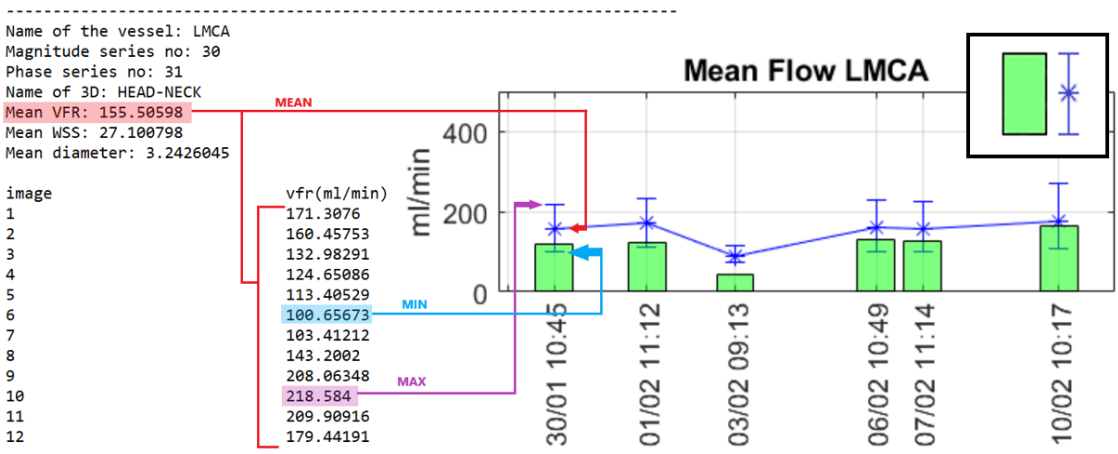

Figure 4.3: Visual explanation of range visualization concept.

The two next variations of the seven plot concept are shown in figures 4.4 and 4.5. Figure 4.4 shows varying ways of using a colorbar to complement the plot in different ways. The main idea with the colorbar is to get a quick overview of the data as the colors corresponding to certain values are shown either in the plot itself, as seen on the left and right side of figure 4.4, or as a guide on the side of the plot as seen in the middle. Colorbars, or color coordination in general, could be used to indicate values or intervals in which one should pay more attention and potentially act upon. The final variation of the seven plot concept, as for the early stage of the project, combines flow and velocity in the same plot, as seen in figure 4.5. As it might be relevant to compare how flow and velocity changes for the same vessel this way of visualizing the data would provide such an option. This visualization does however require two different scales on the vertical axes as flow and velocity have different units but also due to their values lying in different ranges.

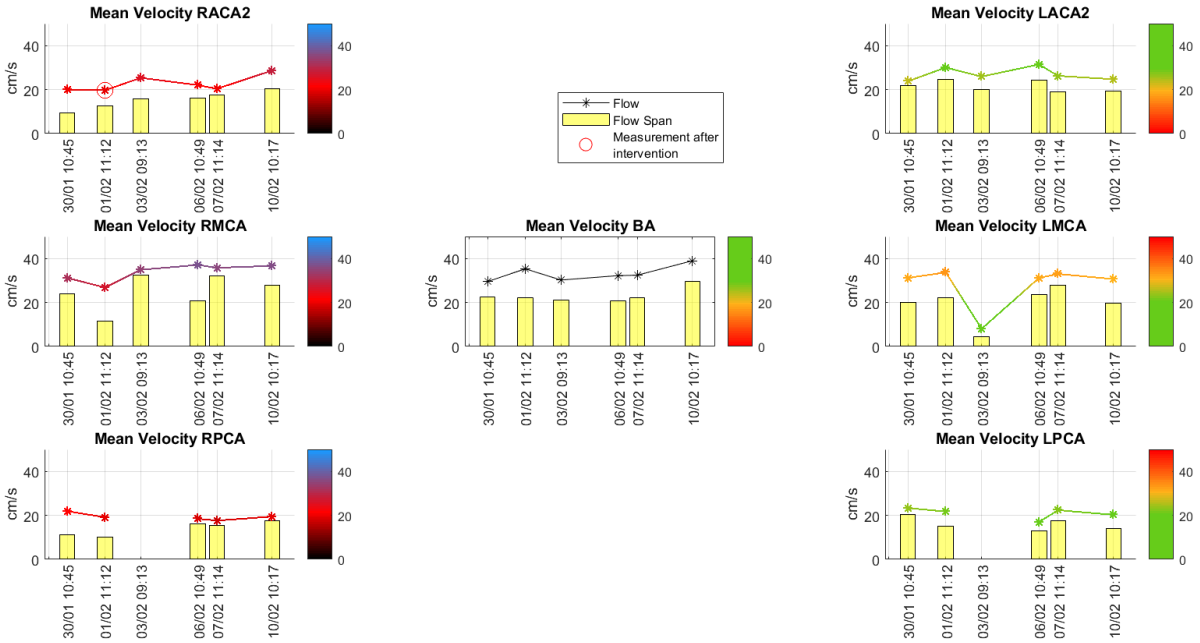

Figure 4.4: Seven plot in one, visualizing mean velocity together with variations of colorbar usage to complement the plot, including different color orders in the colorbar.

Different ways of visualizing inflow and its components are shown in figure 4.6. Bars and plots are used together and separately to show how the same information can be viewed in multiple ways based on which preferences and opinions exist.
The final plot from the early stages of the project is seen in figure 4.7, where the Lindegaard ratio described in section 2.6.1 is visualized. The plot shows two options regarding how background colors could be used. First a more discrete option and second a more continuous option, both including a cut-off value of 3. As a Lindegaard ratio of 3 could be seen as a limit for different interpretations based on whether the ratio is above or below 3 [27], this was chose as the cut-off value.

Mean velocity was used during the early stages of the project and is what is seen in all plots referring to velocity in this section, whereas maximum velocity is what is referred to in section 4.2 when referring to velocity.

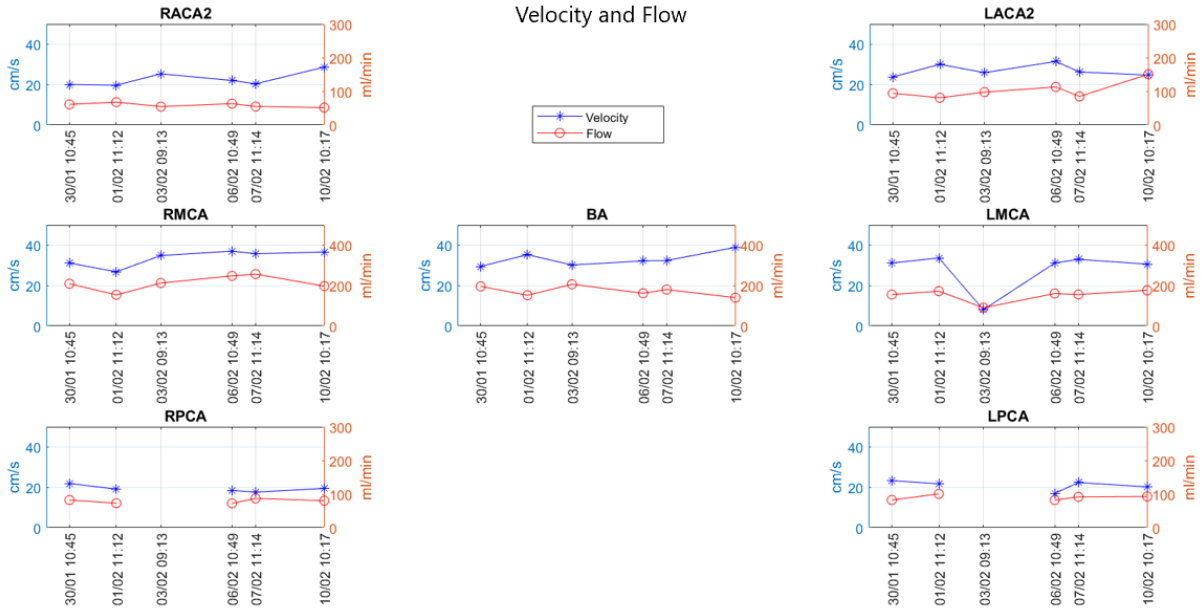

Figure 4.5: Seven plot in one, visualizing flow together with velocity.

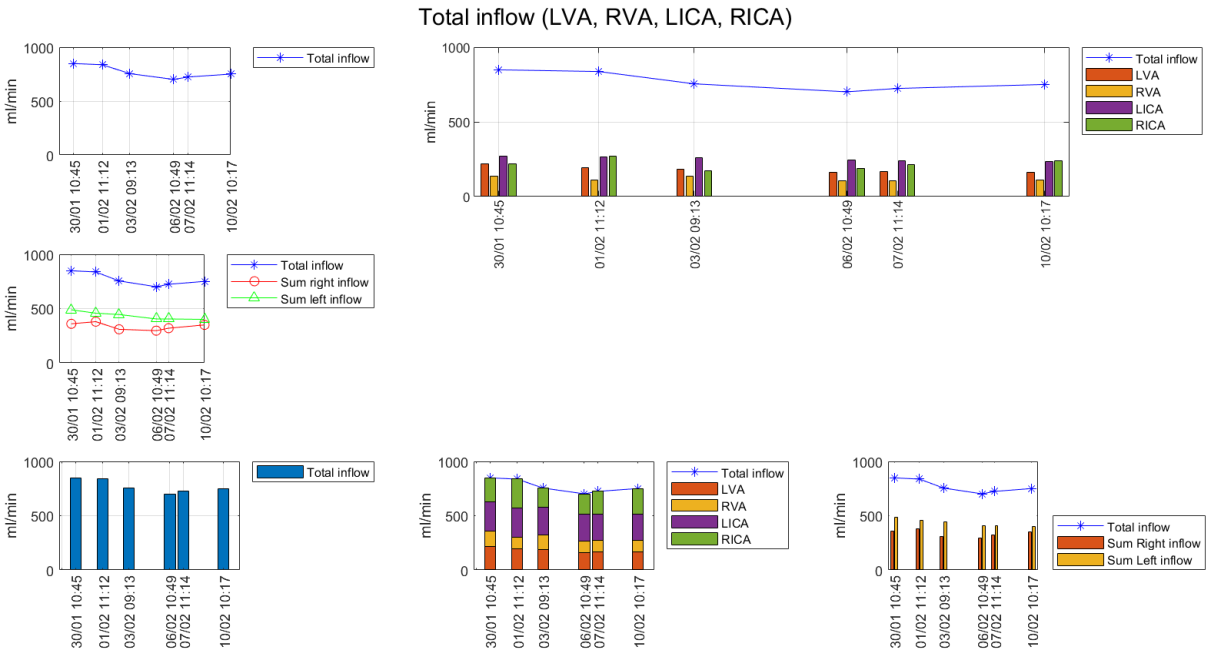

Figure 4.6: Visualization of inflow and its components.

4.2 Graphical User Interface (GUI)

A Graphical User Interface (GUI) was developed in the later stages of the project to gather all visualizations in one place. As can be seen in this section, some components from the plots of the earlier stages of the project, described in the previous section, were slightly adjusted while new components were added based on feedback from supervisors and the neurosurgeons. The final GUI consists of four tabs. The first tab, which works as the initial window

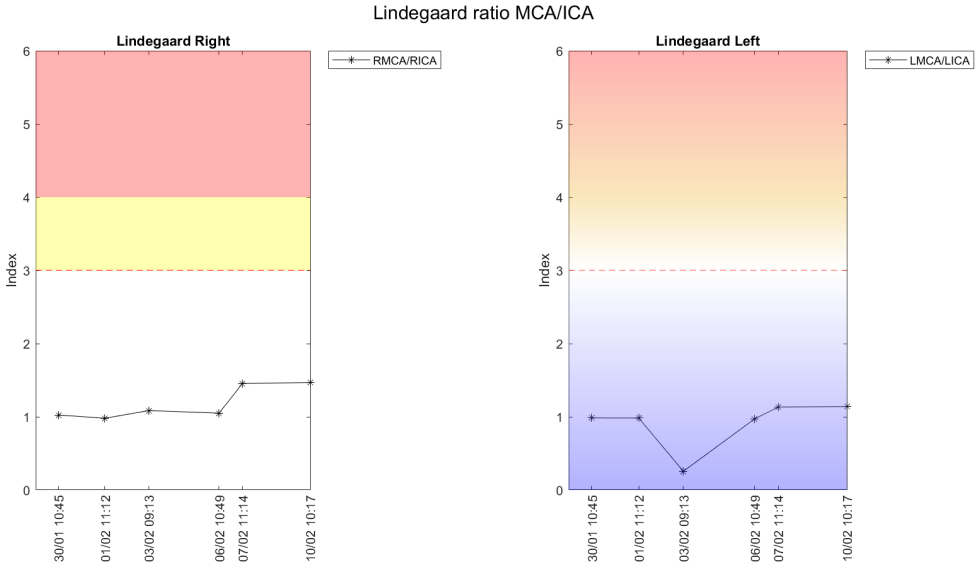

Figure 4.7: Visualization of Lindegaard ratio for left and right side.

a user encounters when using the GUI, is called *Patient and dates* is seen in figure 4.8. As seen, the tab contains two steps to get started with the GUI, the second one being optional. The first step is performed by using the button *Load patient* to navigate to the computers file manager in order to choose which file the measurements should be read from. Once the file has been chosen the second step would be to pick the date of when the SAH occurred. As seen in figure 4.8 a date picker will appear from the date menu and a date can be selected. When the date is set, a table of each measurement date and time is shown along with how many days have passed counting from the day of SAH, as seen in figure 4.9.

The second tab, named *All Vessels*, consist of both a 2D generic vessel map and an extended version of the previously mentioned seven plot concept. Figure 4.10 presents the first view of the second tab. The top of the tab has a text box where the chosen patient file can be seen. The 2D vessel map has multiple options, the first one being if analysis of the flow data or maximum velocity data should be seen. This is controlled with the toggle buttons with the header *Vessel Map View*. Below the toggle buttons there is a drop down menu, containing two options for each respective view. Depending on the choice of analysis option the vessels on the vessel map will be color coded to the corresponding value on the colorbar seen to the, right of the 2D vessel map, based on what calculations were made. The first, and default option, for the Flow view is to see *change in ml/min since last measurement*. Meaning that the color shown in the map will correspond to the difference between the latest and penultimate measurement according to the colorbar. The drop down menu for the Flow view is seen in figure 4.11.

The second option for the Flow view is to visualize the percentage change between the latest measurement and the mean of all previous existing measurements. When this option is chosen the colorbar changes, as well as the range of values for this visualization, as seen in figure 4.12.

For the Velocity view the default option is *change in cm/s since last measurement* as seen in figure 4.13, which is the corresponding option described previously for the Flow view. The velocity values compared consist of the maximum value from the maximum velocity column for the corresponding measurement day. To differentiate between the vessel map options that

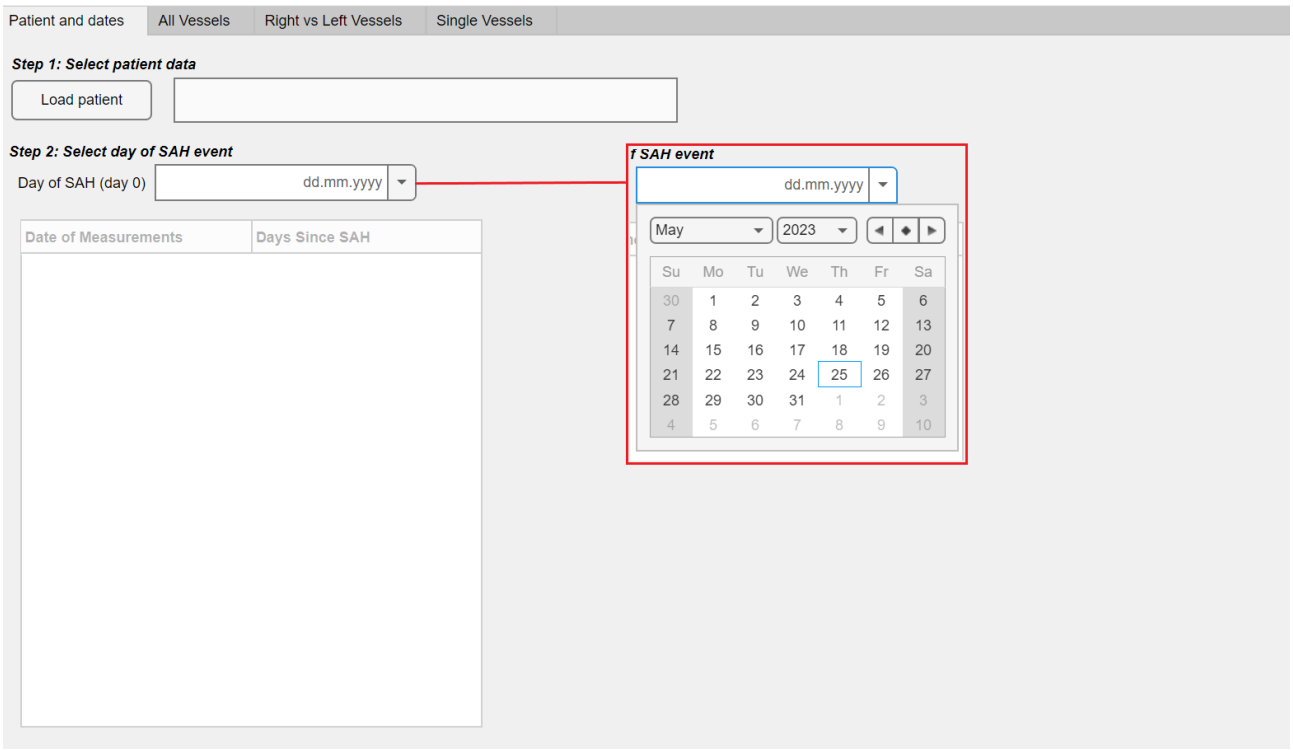

Figure 4.8: Initial view of the first tab of the GUI, before any selections have been made.

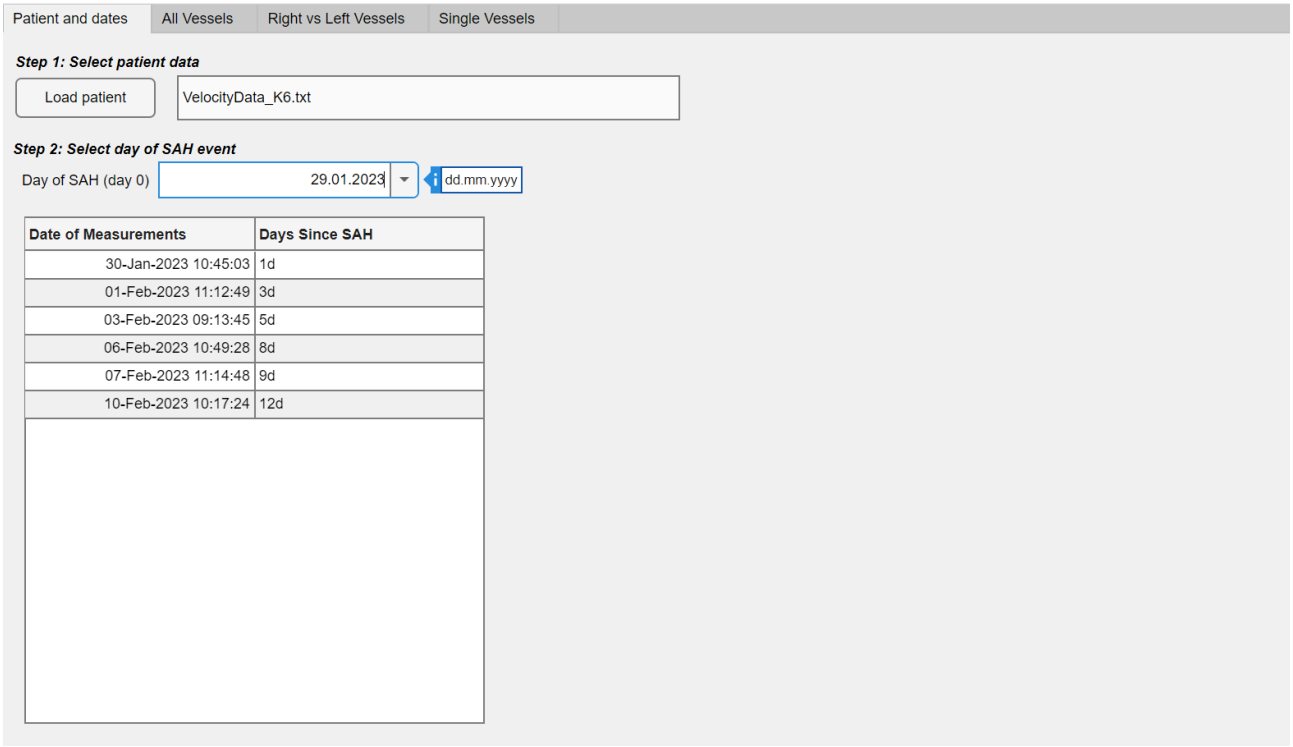

Figure 4.9: Example of the first tab once the file and date of SAH has been picked.

are different for the Flow view and Velocity view different colorbars where chosen. Both the

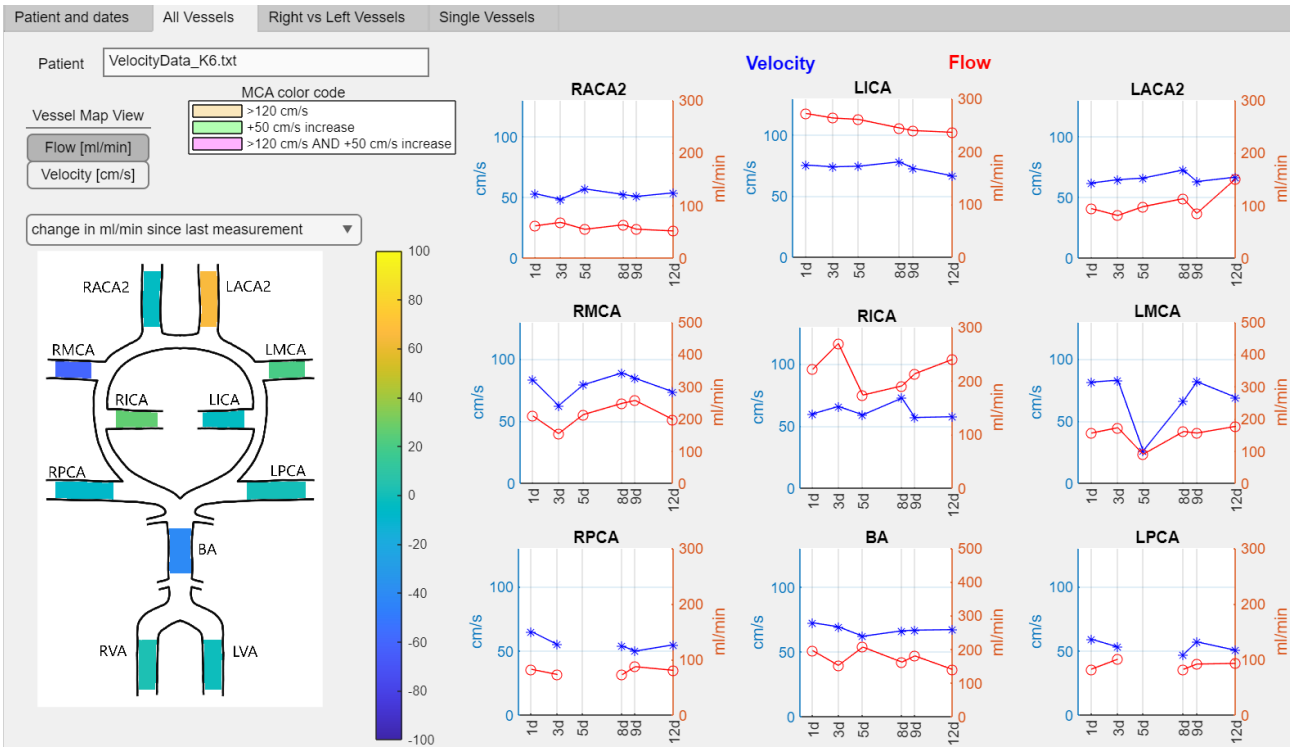

Figure 4.10: First view of the second tab, containing a 2D generic vessel map along with a nine plot setup of flow and maximum velocity visualization.

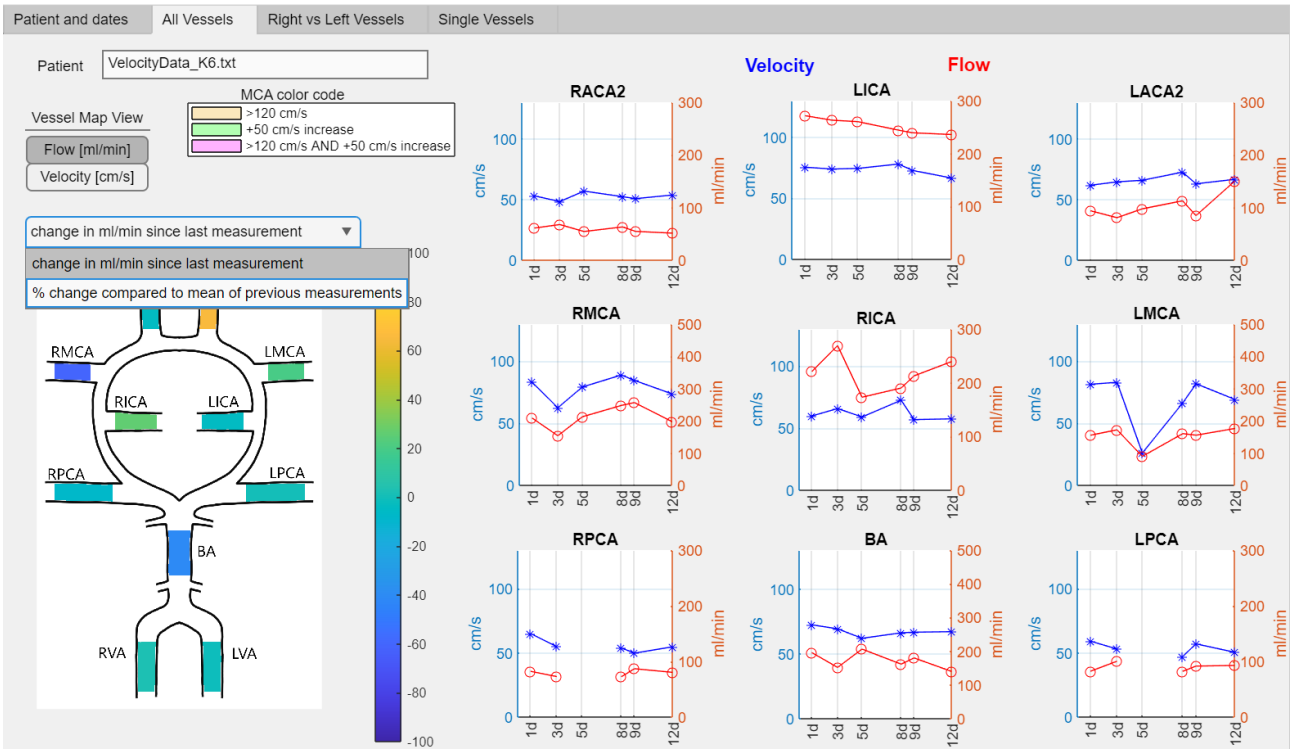

Figure 4.11: Presentation of the drop down menu for the Flow view of the 2D vessel map.

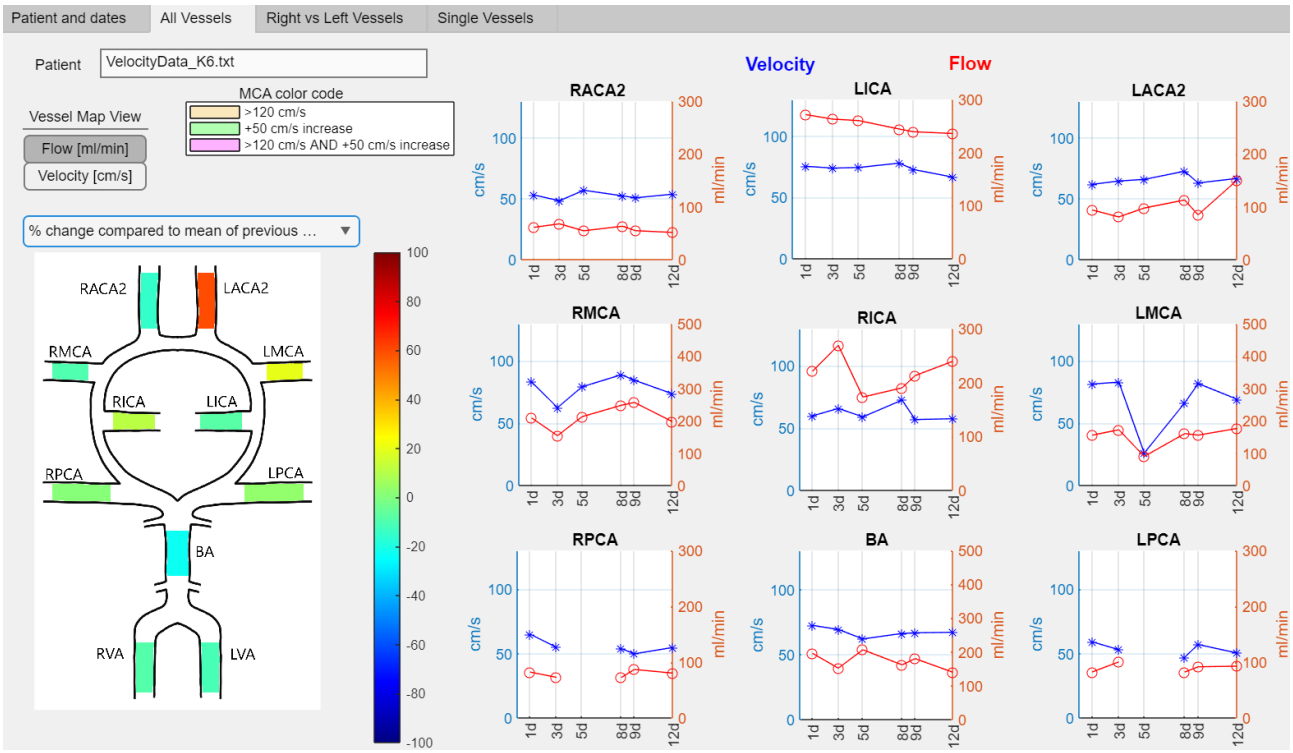

Figure 4.12: Flow view when option to visualize percentage change has been chosen for the 2D vessel map.

Flow view and the Velocity view do however have the same colorbar when the percentage change option is chosen.

As is seen in the second tab, there is a legend with title *MCA color code*. This legend describes what color corresponds to which special case of change in velocity seen in the MCA plots in the nine plot layout. The three cases chosen for this project were if the velocity of the MCA exceeds 120 cm/s, if the velocity has increased with more than 50 cm/s since the previous day and finally if both of those cases occurs at the same time. An example of what this would look like in the middle row of the nine plot setup is shown in figure 4.14.

If one for some reason does not want to pick a date for SAH occurring, or there simply is not one, the difference is seen in what is shown on the horizontal axes of the plots. A case of where no SAH date has been picked is seen in figure 4.15, where the labeling of the horizontal axes now is presented as full dates compared to the abbreviated labeling seen in previous figures.

The third tab, named *Right vs Left Vessels*, is shown in figure 4.16. As in the second tab the third tab contains the text box with the patients filename at the top left. The third tab mainly includes the left and right comparison plots found in the initial plots, as seen in figure 3.4, as well as a shared plot for the Lindegaard ratio for the left and right side.

The fourth and final tab is named *Single Vessels*, and serves as an extra tab where more specific comparisons can be made between all measured vessels. The tab still contains the text box showing the patients filename. The main component of the tab is the vessel selection boxes and the plot area. An example where LACA2 and RACA2 have been chosen is seen in figure 4.17. As the chosen vessels are changed, the legend to the right of the plot is adapted. A second case is seen in figure 4.18. All the different vessels are represented by separate colors

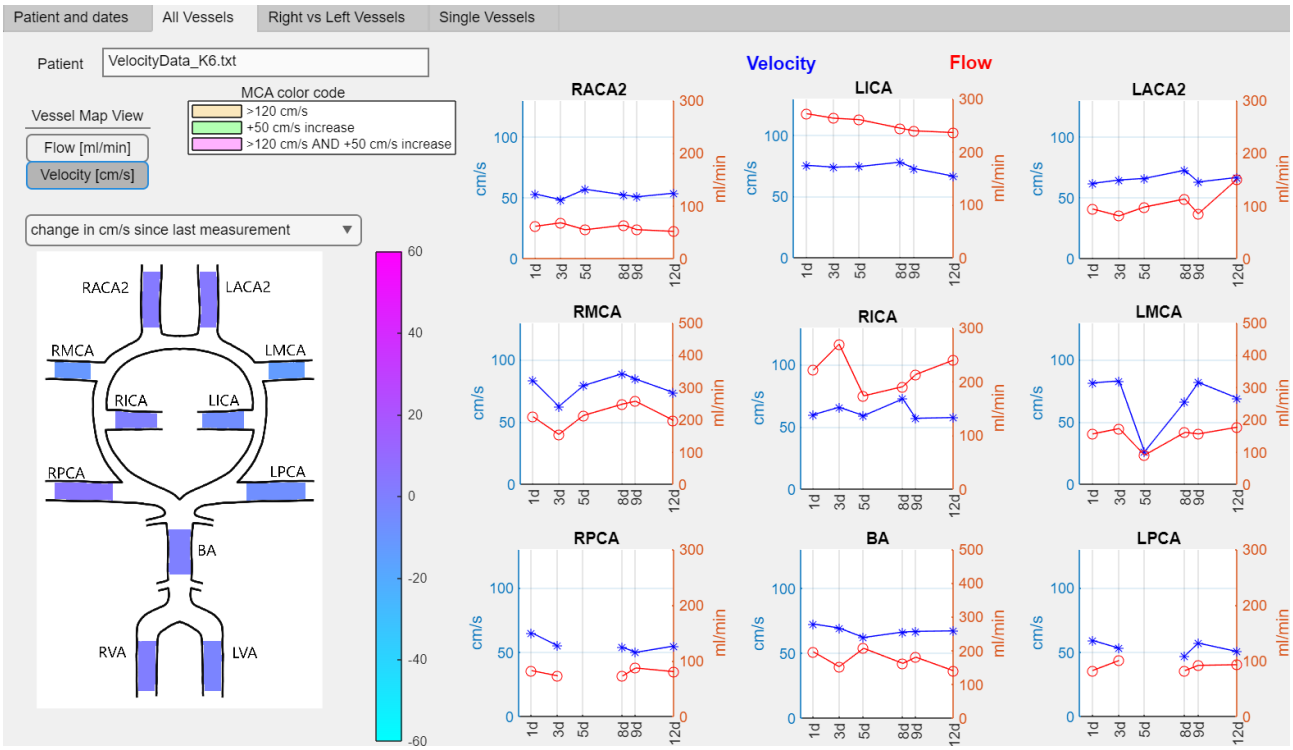

Figure 4.13: Presentation of the drop down menu for the Velocity view of the 2D vessel map.

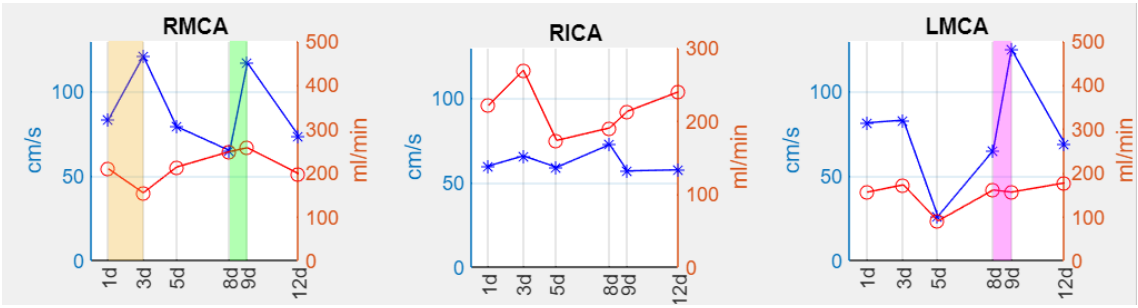

Figure 4.14: Visualization of all three cases analysed further for MCA velocity using the modified data mentioned in chapter 3.4.

and the left and right side of the corresponding vessel is separated by using different plot styles, as seen in the plot legend. The option to clear all selected vessels from the plot is available through the button *Clear All*. Just as for the 2D vessel map found in the second tab, the option to visualize either Flow or Velocity is accessed through the dropdown menu shown in figure 4.19.

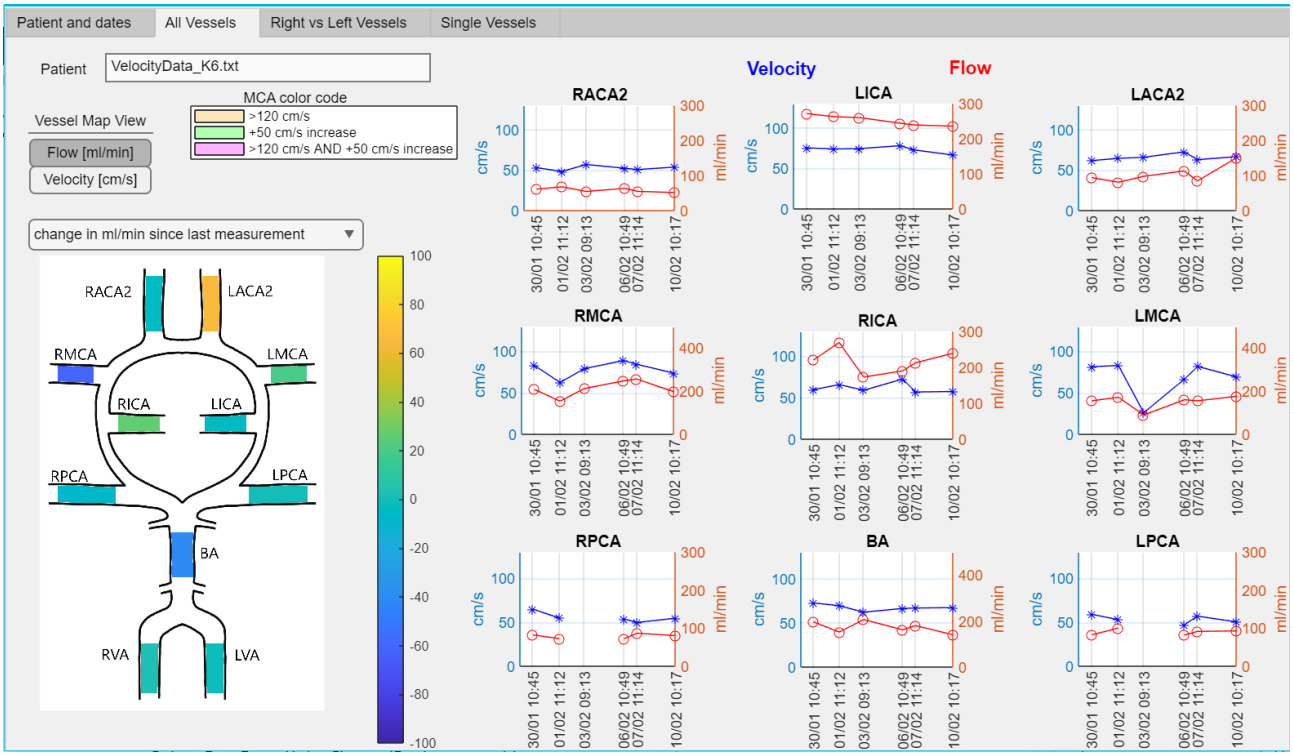

Figure 4.15: Example of second tab where no SAH date has been picked, thus leading to different labeling of the horizontal axes of the plots.

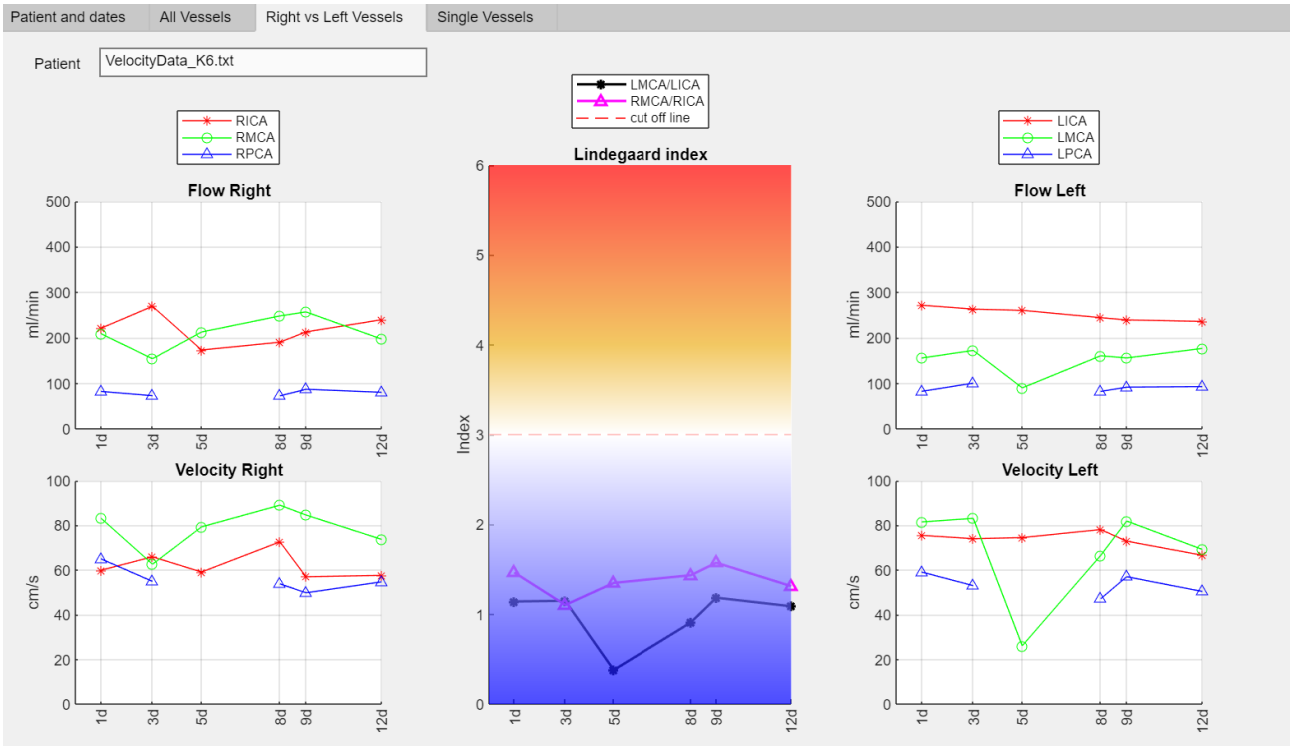

Figure 4.16: Third tab of GUI, including Lindegaards ratio and a simple left and righ side comparison of ICA, MCA and PCA.

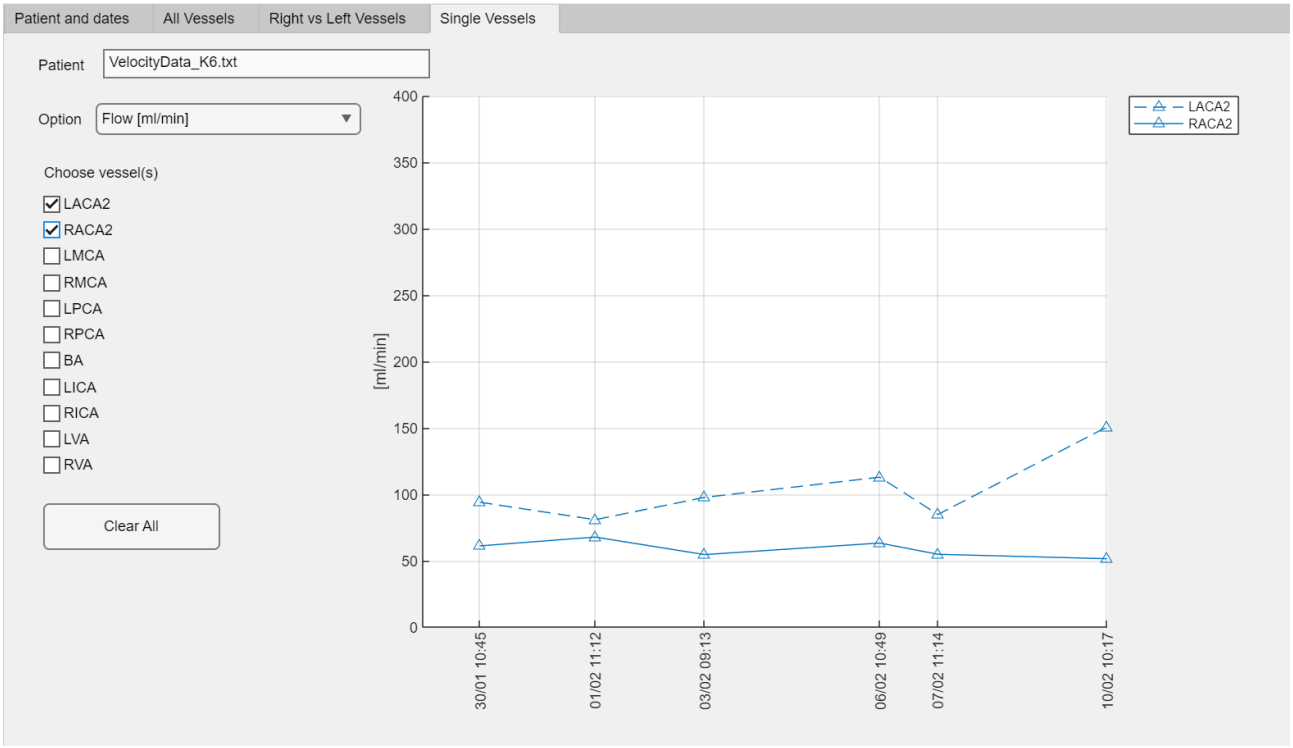

Figure 4.17: Example of selected vessel for visualization, in this case LACA2 and RACA2.

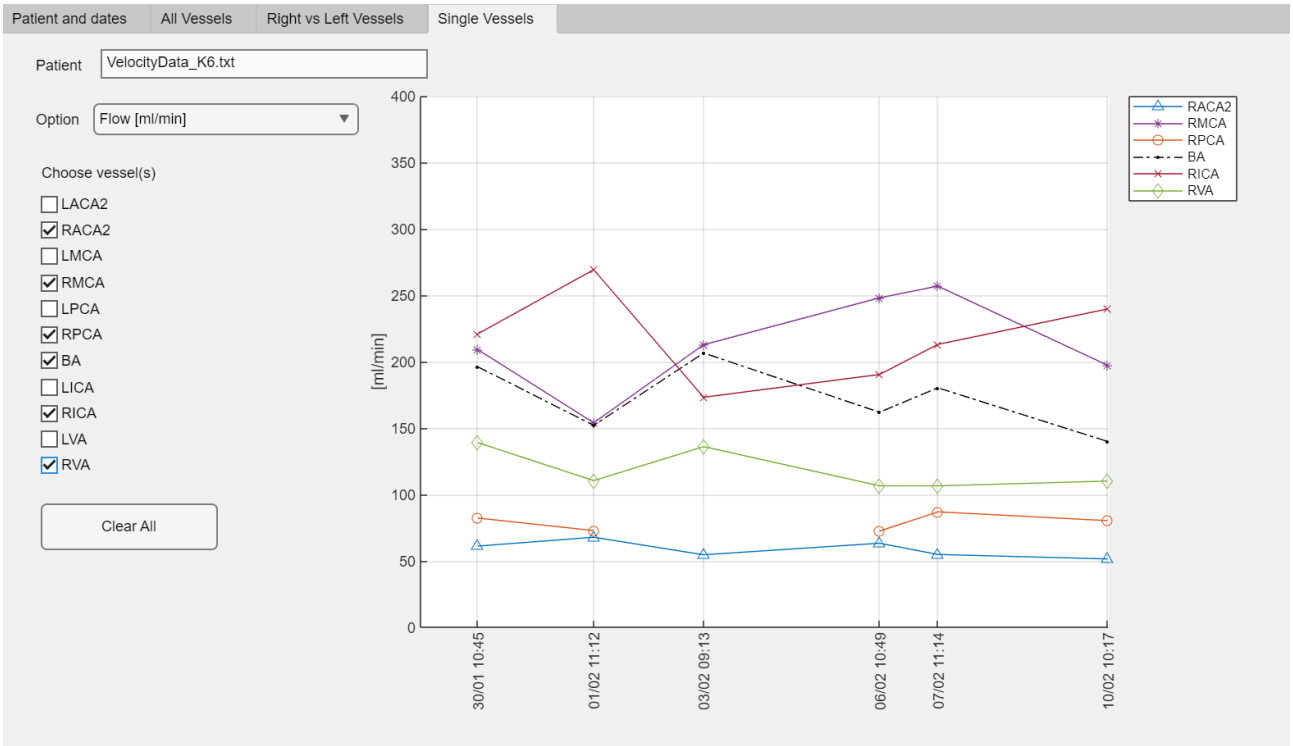

Figure 4.18: Example where multiple vessels have been chosen to be visualized.

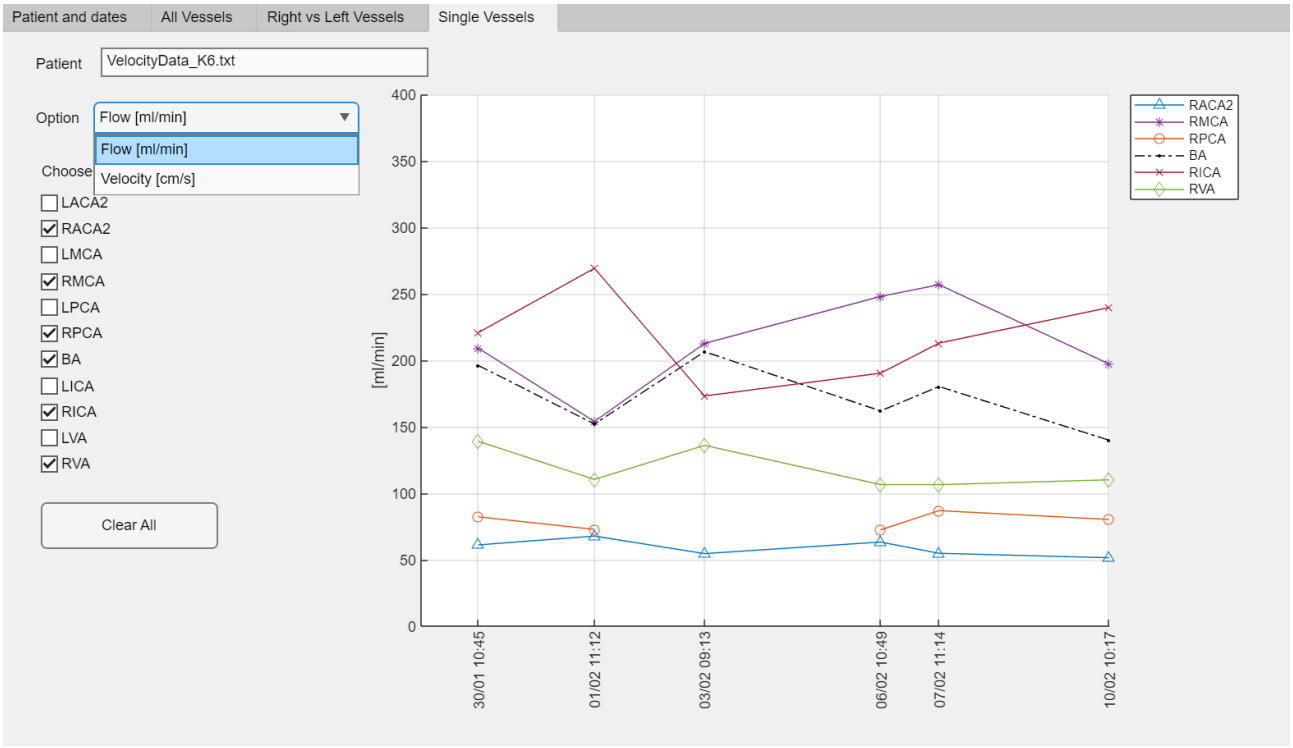

Figure 4.19: Presentation of the dropdown menu and its options for the fourth tab in the GUI.

5 Discussion

A discussion about the data used to develop the visualization and analysis tool, the methodology as well as the obtained results is presented in this chapter. Thoughts on future work is included as well.

5.1 Data

There are both advantages and disadvantages with the data used for this project. The main advantage is how many vessels can actually be measured and studied with the NOVA software and MRI system compared to for instance TCD. As NOVA and MRI allow for more information to be obtained through repeated measurements, without increasing the risk of an increased radiation dose as other methods do, it is worth to keep developing the use of the method. As the data collection requires a notable amount of time to be performed there might be patients for whom the data analysis is not accessible. Patients need to be stable enough to manage the entire image acquisition time and preferably over consecutive days to be able to compare measurements. Since vasospasm begins and develops within a few days following the SAH [13], it is important to keep collecting data from both patients and healthy volunteers to gain more knowledge of what changes can be seen during these days.

As the NOVA software still is under the process of slowly being incorporated into clinical use at the NICU in Linköping University Hospital, the consistency between measurements given different operators has room for improvement. Since new MR technicians continuously need to be trained to operate the NOVA software there is a learning curve within each individual's process just as much as the hospital as whole has to strive for consistency throughout longitudinal measurements. To be able to compare data in a reliable way it is of importance to strive for measurements being comparable by knowing that the conditions in which they were made, here mostly regarding the NOVA operator, are as similar as reasonably possible.

The amount of data from healthy participants to create synthetic data and work on development of the analysis and visualization tool with cases not present in the patients and volunteers currently available has been shown in this thesis to be possible.

5.2 Methodology

The provided initial plot turned out to be a good base for the developed GUI, both regarding content but also layout. To have an initial meeting with the neurosurgeons early in the process was beneficial in the sense that one could begin to understand what could be a useful approach of visualization and analysis from the perspective of a clinician regarding the topic of longitudinal MR measurements. The chosen analysis methods and parameters can be deemed a good starting point for a future project in this field as the increased usage of the NOVA system will yield new ideas and experiences on what the data can be used for and how. The input and feedback provided by the neurosurgeons were of great guidance for the development of the analysis and visualization tool. The feedback aspect of the process was thereby at the end of the project still considered one of the most important factors for the project's development.

5.3 Results

As could be seen in chapter 4, there were adjustments and changes of different degrees between the initial state of the project and the final GUI. The main difference would be the use of maximum velocity instead of mean velocity. Maximum velocity, and especially the maximum value taken from the maximum velocity column, would be more consistent regarding what is actually measured as it is dependent on the highest pixel value found in the area of the vessel in the image. If mean velocity would be used there is a larger dependency on how the operator manually makes adjustments to the marked vessel area, as seen in figure 2.12. Choosing to instead include the maximum value of the maximum velocity column would thus minimize the effect of operator variability. The initial state of exploring plotting possibilities with more of the available data turned out to be beneficial. Together with the feedback it would provide insights on what was useful from the initial state going forward just as much as what was considered unnecessary or even unhelpful in the analysis and visualization method. An example of a component considered unnecessary as seen in the initial plots where the two options to visualize the range of values seen in both the flow and velocity column data. Removing that plotting option provided a less distracting final plot with more focus on the remaining data being showed.

The final GUI provided an accessible way of presenting the NOVA data. The incorporation of a 2D vessel plot provides the opportunity for a quick overview by being guided by the color coding from the colorbar and should be seen as a starting point to what potential lies in this kind of visualization being incorporated. The choice of visualizing the change in either velocity or flow since the previous measurement was done with the idea of the user getting a quick overview of the overall values before potentially diving deeper into the plot of a certain vessel. The other view option, percentage change compared to mean of all previous measurements, was chosen with the purpose of exploring different analysis methods. A comparison between a current value and the mean of all previous could provide a quick overview of how much the current value differs from the overall trend seen from previoues values.

Regarding the 2D vessel map, a concept not prioritized in this project was to explore more in depth how color choices should be used. Factors such as how many colors could be relevant or even necessary to use in a colorbar for a 2D vessel map, or if the colorbar should have a continuous look or discrete look would be relevant to look into further. A discrete colorbar with definite color divisions would remove the possible subjectivity applied by physicians looking at the colors presented for each vessel in the 2D vessel map, whether the subjectivity

is conscious or not. That would thus be a positive aspect of using a discrete colorbar instead.

The current knowledge on what to look for during blood velocity monitoring is noticeably broader than the knowledge on what information blood flow measurements could provide. An example being the previously mentioned guideline values for MCA velocity and changes to velocity [28]. As ways to measure and monitor blood flow increase in availability, the need of more experience in what changes in blood flow and certain values for blood flow could tell us will be important. Experience which could be gained by a larger base of collected data from varying states and conditions.

5.4 Future work

Future work would include further possibilities to adapt thresholds, limits seen in plots and visualization options to suit the user's needs. Investigating how 4D flow MRI data can be visualized together or instead of the 2D phase contrast would be a relevant path forward given the different characteristics of the two techniques. As the thesis was limited to visualizations of lower dimensions, exploring the use of 3D models of the patients vessel structure to visualize the measurements could be relevant. Especially if the possibility to obtain 4D flow MRI data is given. As this thesis explored circulation from a macro perspective with the larger vessels of the brain, the inclusion of micro circulation would be a relevant step forward. One type of measurement to include could be ASL as no contrast agent or radiation is needed and information about brain perfusion is obtained [25]. The inclusion would hopefully provide information useful for the overall picture of the patient's condition. It would be relevant to develop cut-off or reference values for blood flow, as have been seen examples of for velocity. This in order have guidelines for when to intervene or further investigate the patient's state. As with all development of techniques to eventually be used clinically the amount of data acquired would need to be increased in order to study more cases which might relevant to include in the analysis and visualization tool.

6 Conclusion

The result of this thesis presented a tool capable of multiple ways of visualizing and analyzing longitudinal NOVA flow measurements. The developed GUI provided a way to easily interpret the visualizations and analysis. Thus achieving the aim of the thesis. Initial states of the visualizations and analysis provided a good starting point for the project to develop into the final GUI. During the development process feedback from supervisors and neurosurgeons was especially valuable. Variations of plots and a 2D vessel map became the main components of the final tool. Further work within this field could include further development of the adaptability of the visualization and analysis tool. Greater adaptability could open possibilities for new areas of use not initially thought of. Looking into the possibility of using 3D structures as part of the visualization and analysis tool is a path which should be explored. Future work could also include development of MR flow based cut off values to be used together with the tool to indicate when treatment of secondary ischemic events should occur. Other analysis measures and calculations should be explored to expand the information which the tool can provide. A larger collection of data from both healthy volunteers and patients would be useful in the continued development of a tool with the purpose to be used for analysis and visualization.

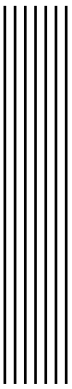

Bibliography

[1] Cleveland Clinic. *Subarachnoid Hemorrhage (SAH)*. URL: https://my.clevelandclinic.org/health/diseases/17871-subarachnoid-hemorrhage-sah (visited on 05/13/2023).

[2] Cleveland Clinic. *Ischemic Stroke*. URL: https://my.clevelandclinic.org/health/diseases/24208-ischemic-stroke-clots (visited on 05/21/2023).

[3] Nadine Barrie Smith and Andrew Webb. *Introduction to Medical Imaging*. Cambridge University, 2011.

[4] Katherine H. Taber Ph.D., Jana G. Zimmerman Ph.D., Howard Yonas M.D., William Hart B.S.R.S. R.T., and Robin A. Hurley M.D. "Applications of Xenon CT in Clinical Practice: Detection of Hidden Lesions". In: (1999). URL: https://doi.org/10.1176/jnp.11.4.423.

[5] Daniel Václavík, Ondrej Volný, Petra Cimflová, Krystof Švub, Katerina Dvorníková, and Michal Bar. "The importance of CT perfusion for diagnosis and treatment of ischemic stroke in anterior circulation". In: (2022). DOI: 10.31083/j.jin2103092.

[6] Johns Hopkins Medicine. *Brain Anatomy and How the Brain Works*. URL: https://www.hopkinsmedicine.org/health/conditions-and-diseases/anatomy-of-the-brain (visited on 05/28/2023).

[7] Dale Purves, George J Augustine, David Fitzpatrick, Lawrence C Katz, Anthony-Samuel LaMantia, James O McNamara, and S Mark Williams. *Neuroscience*. 2nd Edition. Sunderland (MA): Sinauer Associates, 2001. Chap. The Blood Supply of the Brain and Spinal Cord. URL: https://www.ncbi.nlm.nih.gov/books/NBK11042/ (visited on 05/14/2023).

[8] Brit Long, Alex Koyfman, and Michael S. Runyon. "Subarachnoid Hemorrhage: Updates in Diagnosis and Management". In: *Emergency Medicine Clinics of North America* 35.4 (2017), pp. 803–824. ISSN: 0733-8627. DOI: https://doi.org/10.1016/j.emc.2017.07.001. URL: https://www.sciencedirect.com/science/article/pii/S0733862717300603.

[9] The National Health Service. *Causes*. URL: https://www.nhs.uk/conditions/subarachnoid-haemorrhage/causes/ (visited on 05/13/2023).

[10] Alkhachroum Ayham, Megjhani Murad, Terilli Kalijah, Rubinos Clio, Ford Jenna, Wallace Brendan K, Roh David J, Agarwal Sachin, Connolly E Sander, Boehme Amelia K, et al. "Hyperemia in subarachnoid hemorrhage patients is associated with an increased risk of seizures". In: *Journal of Cerebral Blood Flow & Metabolism* 40.6 (2020), pp. 1290–1299.

[11] Hawryluk Gregory WJ, Citerio Giuseppe, Hutchinson Peter, Kolias Angelos, Meyfroidt Geert, Robba Chiara, Stocchetti Nino, and Chesnut Randall. "Intracranial pressure: current perspectives on physiology and monitoring". In: *Intensive Care Medicine* 48.10 (2022), pp. 1471–1481.

[12] The National Health Service. *Treatment*. URL: https://www.nhs.uk/conditions/subarachnoid-haemorrhage/treatment/ (visited on 05/13/2023).

[13] Philippa Newfield. "Chapter 179 - Intracranial Aneurysms: Vasospasm and Other Issues". In: *Complications in Anesthesia (Second Edition)*. Ed. by John L. Atlee. Second Edition. W.B. Saunders, 2007, pp. 719–723. ISBN: 978-1-4160-2215-2. DOI: https://doi.org/10.1016/B978-1-4160-2215-2.50184-8. URL: https://www.sciencedirect.com/science/article/pii/B9781416022152501848.

[14] Asad Ikram, Muhammad Ali Javaid, Santiago Ortega-Gutierrez, Magdy Selim, Sarah Kelangi, Syed Muhammad Hamza Anwar, Michel T. Torbey, and Afshin A. Divani. "Delayed Cerebral Ischemia after Subarachnoid Hemorrhage". In: *Journal of Stroke and Cerebrovascular Diseases* 30.11 (2021), p. 106064. ISSN: 1052-3057. DOI: https://doi.org/10.1016/j.jstrokecerebrovasdis.2021.106064. URL: https://www.sciencedirect.com/science/article/pii/S1052305721004699.

[15] David A. Rubenstein, Wei Yin, and Mary D. Frame. *Biofluid Mechanics*. Academic Press, 2021. URL: https://doi.org/10.1016/C2018-0-02144-1.

[16] Lee Waite and Jerry Fine. *Applied Biofluid Mechanics*. McGraw-Hill Professional Publishing, 2007.

[17] Donald W. McRobbie, Elizabeth A. Moore, Martin J. Graves, and Martin R. Prince. *MRI from Picture to Proton*. 2nd edition. Cambridge University Press, 2006.

[18] Brian M. Dale, Mark A. Brown, and Richard C. Semelka. *MRI : basic principles and applications.* Wiley Blackwell, 2015. ISBN: 9781119013051.

[19] Questions and Answers in MRI. *Phase-Contrast MRA*. URL: https://www.mriquestions.com/phase-contrast-mra.html (visited on 05/28/2023).

[20] Gilles Soulat, Patrick McCarthy, and Michael Markl. "4D Flow with MRI". In: *Annual Review of Biomedical Engineering* 22.1 (2020), pp. 103–126. DOI: 10.1146/annurev-bioeng-100219-110055. eprint: https://doi.org/10.1146/annurev-bioeng-100219-110055. URL: https://doi.org/10.1146/annurev-bioeng-100219-110055.

[21] Tomas Vikner, Lars Nyberg, Madelene Holmgren, Jan Malm, Anders Eklund, and Anders Wåhlin. "Characterizing pulsatility in distal cerebral arteries using 4D flow MRI". In: *Journal of Cerebral Blood Flow & Metabolism* 40.12 (2020), pp. 2429–2440. DOI: 10.1177/0271678X19886667. eprint: https://doi.org/10.1177/0271678X19886667. URL: https://doi.org/10.1177/0271678X19886667.

[22] Madelene Holmgren, Anders Wåhlin, Tora Dunås, Jan Malm, and Anders Eklund. "Assessment of Cerebral Blood Flow Pulsatility and Cerebral Arterial Compliance With 4D Flow MRI". In: *Journal of Magnetic Resonance Imaging* 51.5 (2020), pp. 1516–1525. DOI: https://doi.org/10.1002/jmri.26978. eprint: https://onlinelibrary.wiley.com/doi/pdf/10.1002/jmri.26978. URL: https://onlinelibrary.wiley.com/doi/abs/10.1002/jmri.26978.

[23] Marco Essig, Mark S. Shiroishi, Thanh Binh Nguyen, Marc Saake, James M. Provenzale, David Enterline, Nicoletta Anzalone, Arnd Dörfler, Àlex Rovira, Max Wintermark, and Meng Law. "Perfusion MRI: The Five Most Frequently Asked Technical Questions". In: *American Journal of Roentgenology* 200.1 (2013), pp. 24–34. DOI: 10.2214/AJR.12.9543. eprint: https://doi.org/10.2214/AJR.12.9543. URL: https://doi.org/10.2214/AJR.12.9543.

[24] Jeffrey R. Petrella and James M. Provenzale. "MR Perfusion Imaging of the Brain Techniques and Applications". In: (2000).

[25] Luis Hernandez-Garcia, Anish Lahiri, and Jonas Schollenberger. "Recent progress in ASL". In: *NeuroImage* 187 (2019), pp. 3–16. DOI: https://doi.org/10.1016/j.neuroimage.2017.12.095. URL: https://www.sciencedirect.com/science/article/pii/S1053811917311199.

[26] Inc VasSol. *NOVA® quantifies the blood flow in vessels using standard MRI scanning.* URL: https://vassolinc.com/ (visited on 05/13/2023).

[27] Gyanendra Kumar MD and Andrei V. Alexandrov MD. "Vasospasm Surveillance With Transcranial Doppler Sonography in Subarachnoid Hemorrhage". In: (2015). URL: https://onlinelibrary.wiley.com/doi/abs/10.7863/ultra.34.8.1345.

[28] Navneh Samagh, Hemant Bhagat, and Kiran Jangra. "Monitoring cerebral vasospasm: How much can we rely on transcranial Doppler". In: *J Anaesthesiol Clin Pharmacol* 35 (2019), pp. 12–18.

[29] Cerebral Angiography. *Brain Aneurysm*. URL: https://my.clevelandclinic.org/health/diagnostics/13476-cerebral-angiography#additional-details (visited on 05/28/2023).

[30] RadiologyInfo.org. *CT Angiography (CTA)*. URL: https://www.radiologyinfo.org/en/info/angioct (visited on 05/28/2023).

[31] J. Hillman, P. Sturnegk, H. Yonas, J. Heron, M. Sandborg, T. Gunnarsson, and P. Mellergård. "Bedside monitoring of CBF with xenon-CT and a mobile scanner: a novel method in neurointensive care". In: *British Journal of Neurosurgery* 19.5 (2005), pp. 395–401. DOI: 10.1080/02688690500389898. eprint: https://doi.org/10.1080/02688690500389898. URL: https://doi.org/10.1080/02688690500389898.

7 Appendix- User Manual

7.1 Introduction

This user manual contains information about how to use the GUI developed during the thesis *Development of a tool for analysis and visualization of longitudinal magnetic resonance flow measurements of subarachnoid hemorrhage patients in the neurointensive care unit*.

7.2 Preparation

The necessary files needed to run the GUI include the main MATLAB application file, the base image file for the 2D vessel map as well as the mask image files for each vessel (a total of 11 vessel files). MATLAB needs to be installed on the used computer in order to run the application.

7.3 Input Data

The input data will be measurements from NOVA and all measurements made on a person are expected to be collected into one file and in a specific format seen in figure 7.1. There is a main section for general information marked with red rectangle the where there is a main section and general information about the file is found. Below the general section comes the section that is repeated for every vessel until a new measurement date comes along. It is assumed and expected that at least three measurement dates are present in the input file to use the software.

7.4 Tab 1: Patient and dates

The first tab, as seen in figure 7.2, is where the user selects the patient file to be analysed as well as set the date of when the subarachnoid hemorrhage occurred. The main components in the first tab are the *Load patient* button and the *Day of the day 0* date picker. By choosing a patient file along with a date a list of when all the measurement where done relative the chosen date. The date can be changed. A patient file can be chosen without choosing a date

```
loading ReportObject ...
ReportObject software version: 8.1.1
Vendor: SIEMENS
Patient Name: K6
Patient ID: K6
Study Date/Time: 01/30/2023  10:45:03
Heart Rate: 70
Report Status: APPROVED
Creation Date/Time: 02/03/2023  10:14:55
Approve Date/Time:
# of vessels: 11
```

```
----------------------------------------------------------------------
Name of the vessel: LVA
Magnitude series no: 20
Phase series no: 21
Name of 3D: HEAD-NECK
Mean VFR: -217.0918
Mean WSS: -11.884159
Mean diameter: 4.7701344

image          time_delay(ms) vfr(ml/min)    mean_vel(cm/s) max_vel(cm/s)  min_vel(cm/s)  diameter(mm)    area(mm2)       wss(dynes2/cm2)
1              0.0            -221.6953      -20.12553      -44.4          -20.12553      4.8348613       18.359375       -11.655241
2              74.416664      -204.02347     -18.521278     -41.4          -18.521278     4.8348613       18.359375       -10.726176
3              148.83333      -185.6953      -16.857447     -39.0          -16.857445     4.8348613       18.359375       -9.762604
4              223.25         -165.07033     -15.31087      -36.3          -15.31087      4.7831497       17.96875        -8.962807
5              297.66666      -137.34375     -14.292685     -33.8          -14.292683     4.51572         16.015625       -8.862267
6              372.0833       -131.60158     -13.058141     -32.100002     -13.058141     4.624548        16.796875       -7.9062424
7              446.5          -133.21873     -13.218602     -31.300001     -13.218604     4.624548        16.796875       -8.003397
8              520.9166       -217.40622     -19.736168     -39.8          -19.736168     4.8348613       18.359375       -11.42975
9              595.3333       -334.0078      -30.321276     -56.4          -30.321276     4.8348613       18.359375       -17.559874
10             669.75         -336.8906      -30.582973     -56.4          -30.582977     4.8348613       18.359375       -17.711432
11             744.1666       -294.14066     -26.70213      -54.2          -26.70213      4.8348613       18.359375       -15.463928
12             818.5833       -244.00781     -22.151064     -47.3          -22.151064     4.8348613       18.359375       -12.828283
```

Figure 7.1: Example of input file. The general section which is repeated for every new measurement date is marked with the red rectangle. The blue rectangle represents the vessel component which is repeated for every vessel until a new measurement date begins.

of SAH, which will affect the way the plot axes look like in tab 2 and 3. An example of what tab 1 looks like when both fie and date have been selected is seen in figure 7.3

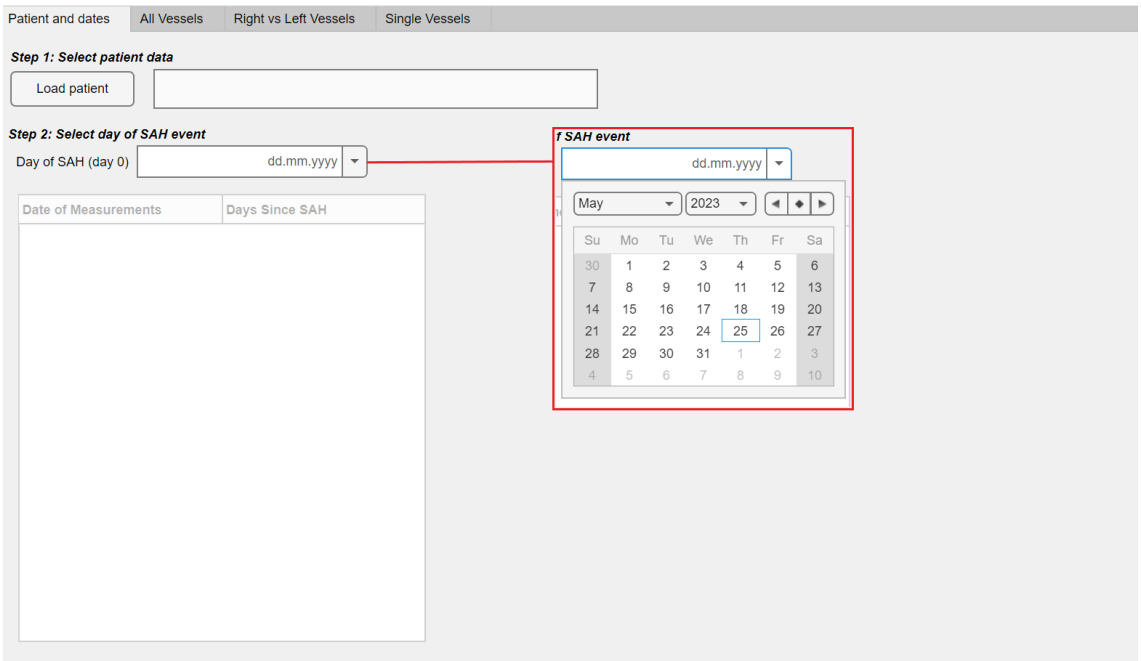

Figure 7.2: Initial view of the first tab of the GUI, before any selections have been made.

7.5 Tab 2: All Vessels

The second tab contains both a nine-plot view of a flow versus velocity comparison can be seen as well as a 2D generic vessel plot. The 2D vessel plot has 4 view options. Two options

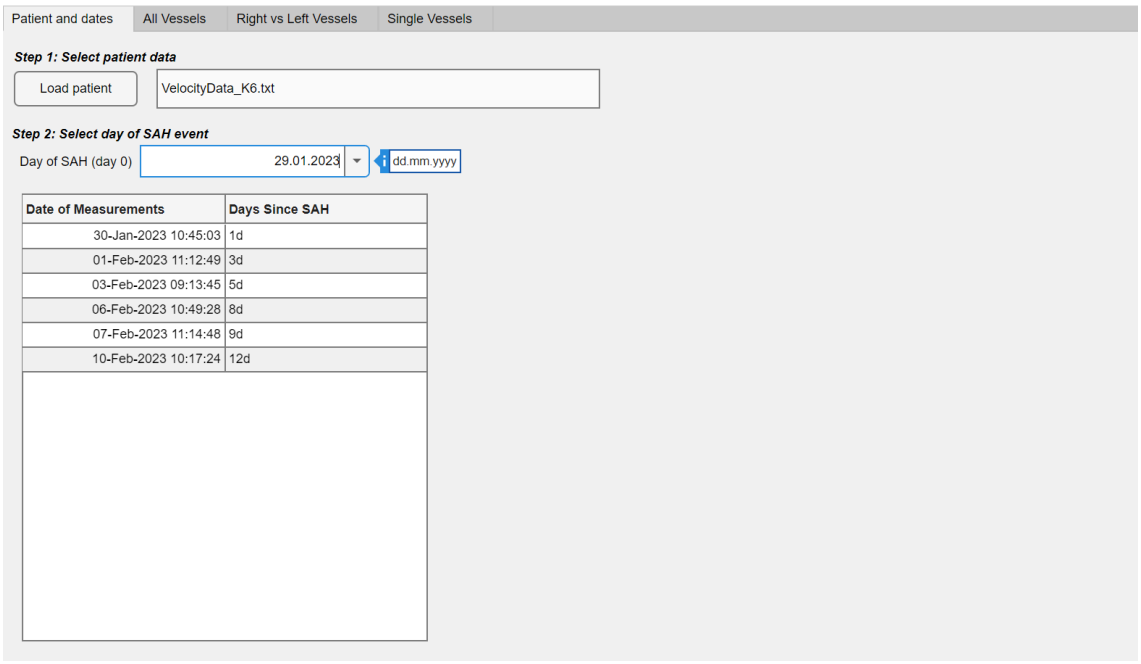

Figure 7.3: Example of both a selected file and a date of SAH event .

for velocity and two for flow. The common view for both is to see the percentage change compared to a mean value calculated from all previous values. An example of what the second tab looks like once a file and date have been picked is seen in figure 7.4.

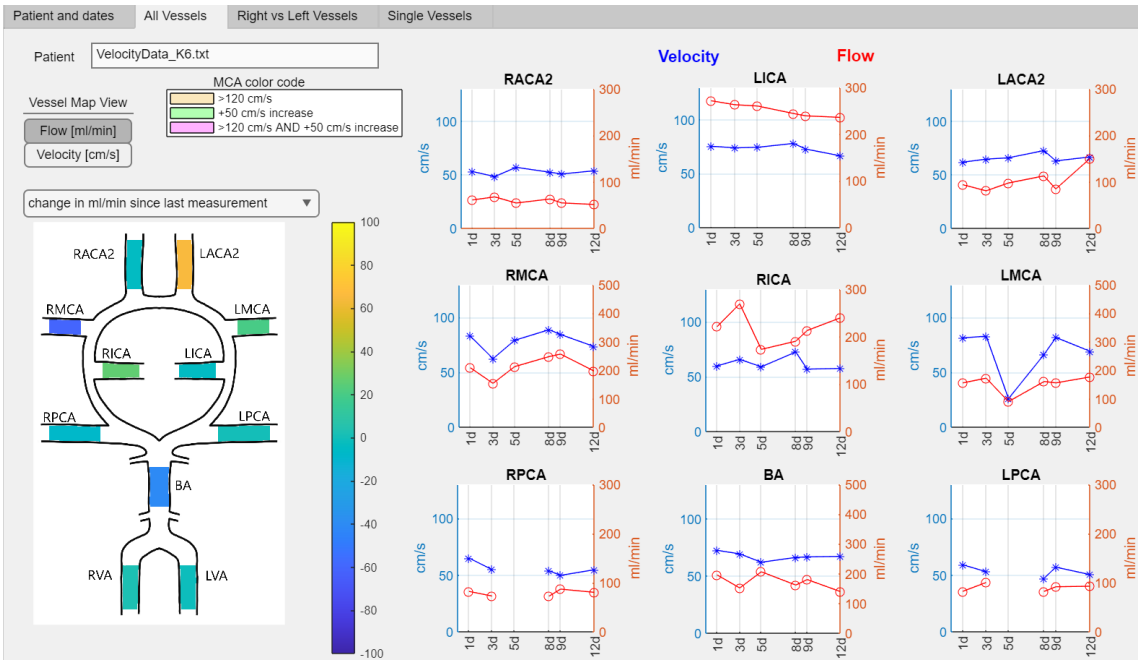

Figure 7.4: First view of the second tab, containing a 2D generic vessel map along with a nine plot setup of flow and maximum velocity visualization.

The second tab contains a legend with extra information about three special cases for MCA which result in an extra visualization component if full filled. A close up of the legend is seen

in figure 7.5, the visualization in the 9 plot setup when one of the three included special cases is present. An example of what each full filled special case looks like in the second tab is seen in figure 7.6.

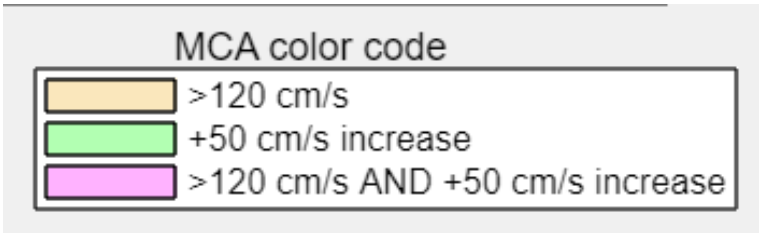

Figure 7.5: Close up of legend in second tab of the GUI.

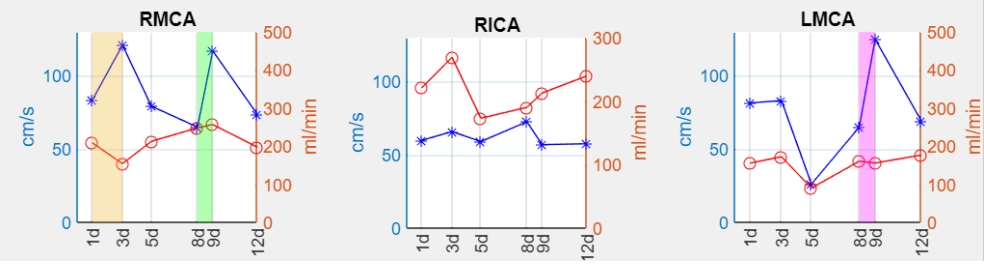

Figure 7.6: Visualization of all three cases analysed further for MCA velocity using the modified data mentioned in chapter 3.4.

To change the 2D vessel map view, a drop down menu is used which can be seen in figure 7.7. Examples of the remaining views for the 2D vessel map of the second tab are seen in figures 7.9 and 7.8.

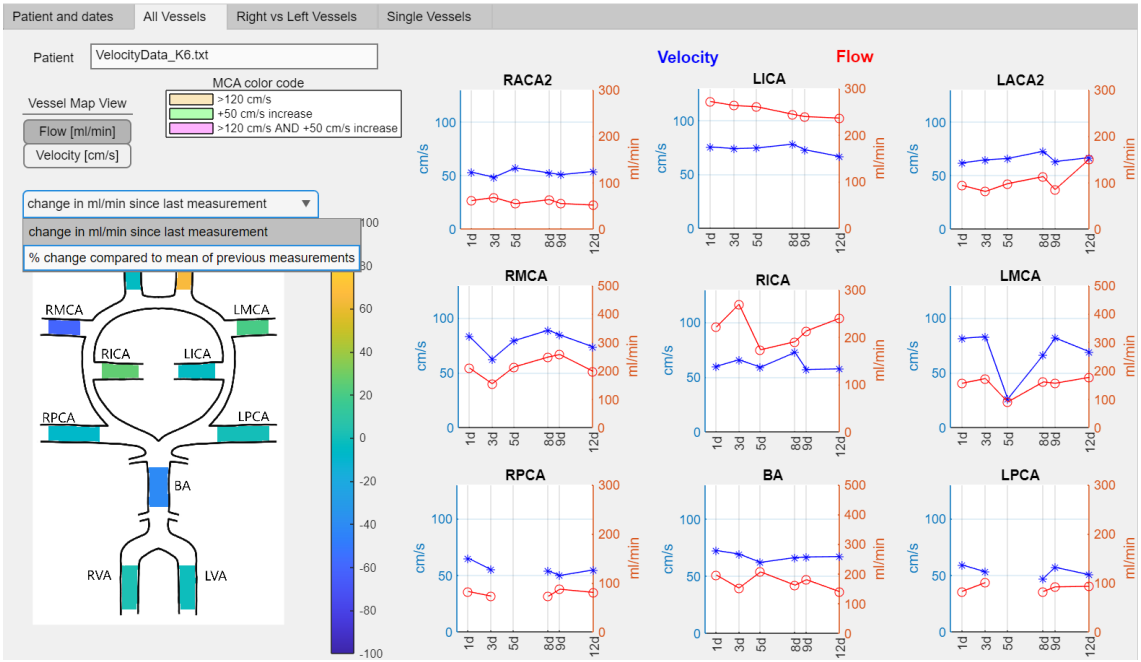

Figure 7.7: Presentation of the drop down menu for the Flow view of the 2D vessel map.

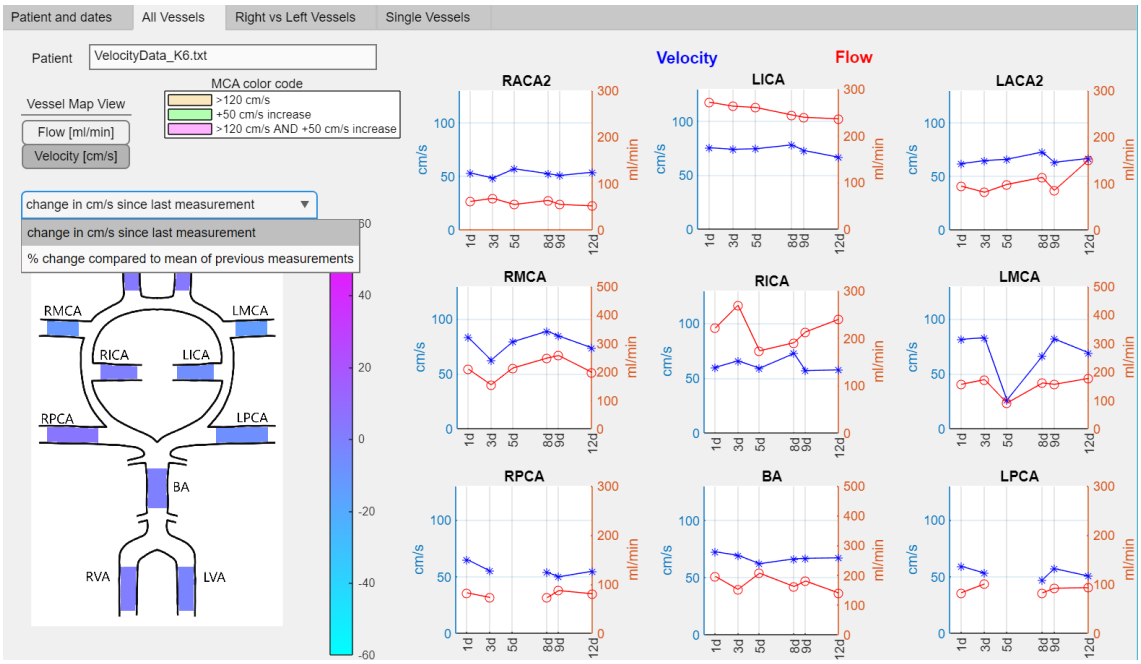

Figure 7.8: Presentation of the drop down menu for the Velocity view of the 2D vessel map.

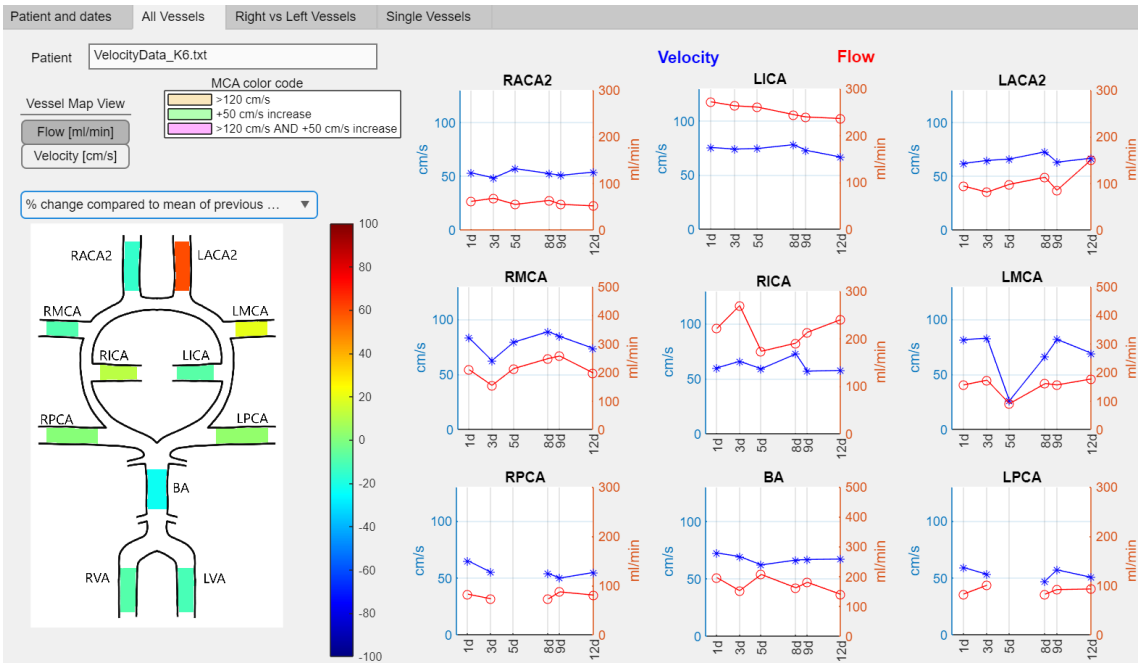

Figure 7.9: Flow view when option to visualize percentage change has been chosen for the 2D vessel map.

If no SAH date has been picked the plots will have the full measurement dates on the horizontal axis of each plot. This is seen as an example in 7.10.

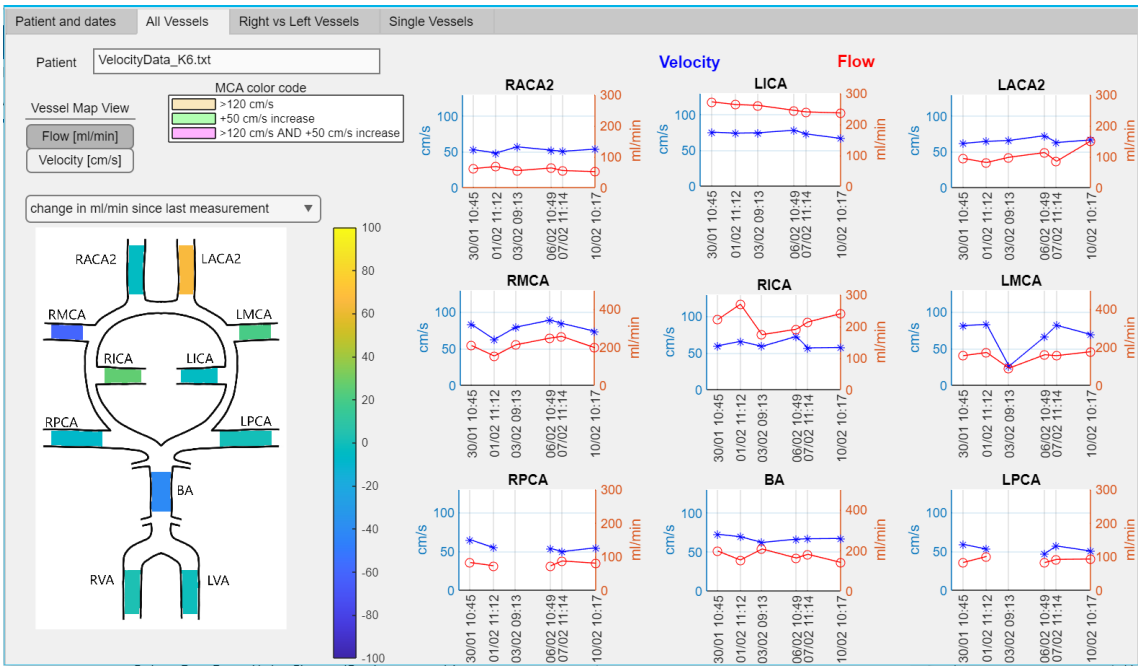

Figure 7.10: Example of second tab where no SAH date has been picked, thus leading to different labeling of the horizontal axes of the plots.

7.6 Tab 3: Right vs Left Vessels

The third tab contains a right versus left comparison where flow and velocity are kept in different plots. There is no interactive component in the third tab. An example of the third tab is seen in figure 7.11.

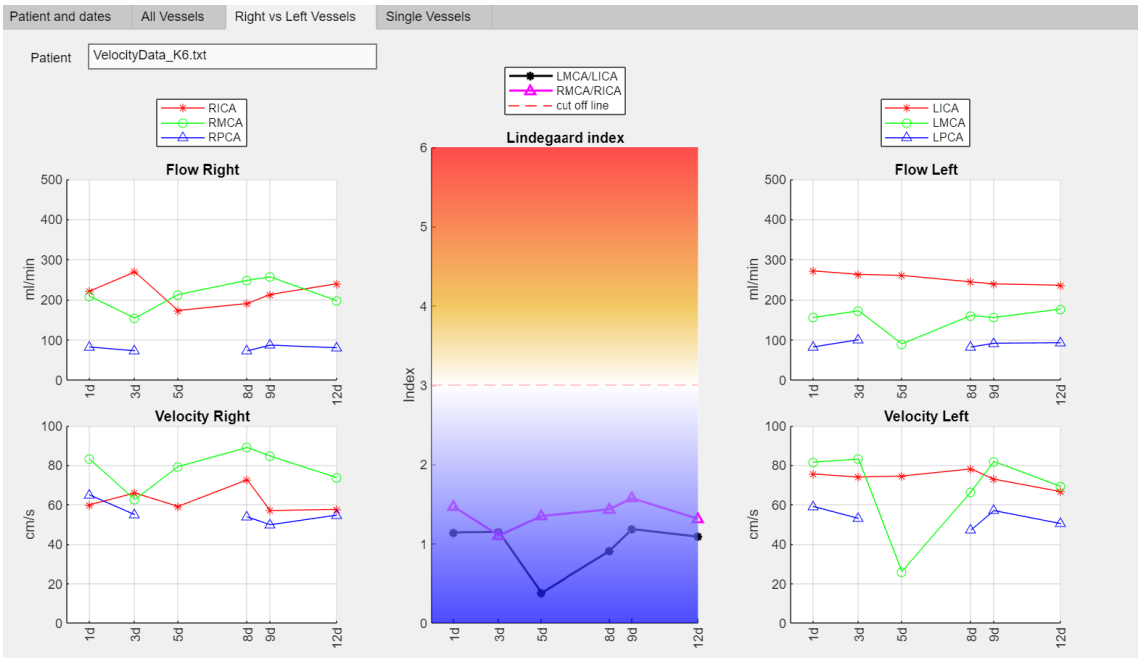

Figure 7.11: Third tab of GUI, including Lindegaards ratio and a simple left and righ side comparison of ICA, MCA and PCA.

7.7 Tab 4: Single Vessels

The fourth tab is meant as a space where it is up to the user decide which vessels are relevant to study more, and whether it should be shown as flow or velocity measurements. The tab also has a Clear All button in order to clear all chosen vessels and clear the plot. Examples of what the fourth tab can look like are seen in figures 7.12, 7.13 and 7.14.

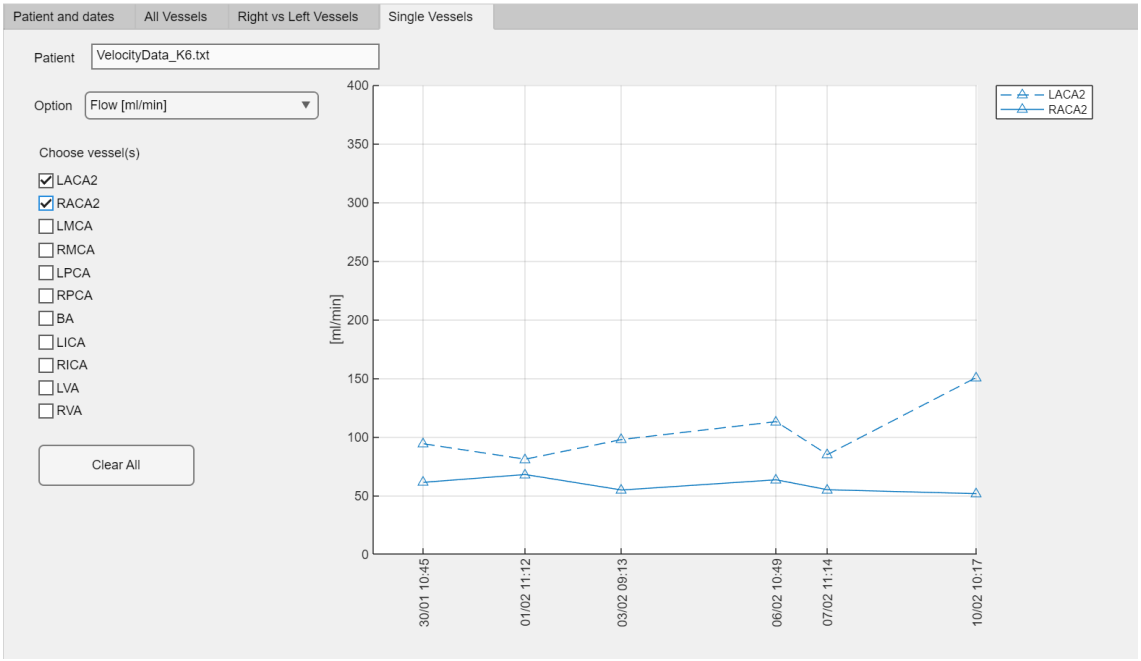

Figure 7.12: Example of selected vessel for visualization, in this case LACA2 and RACA2.

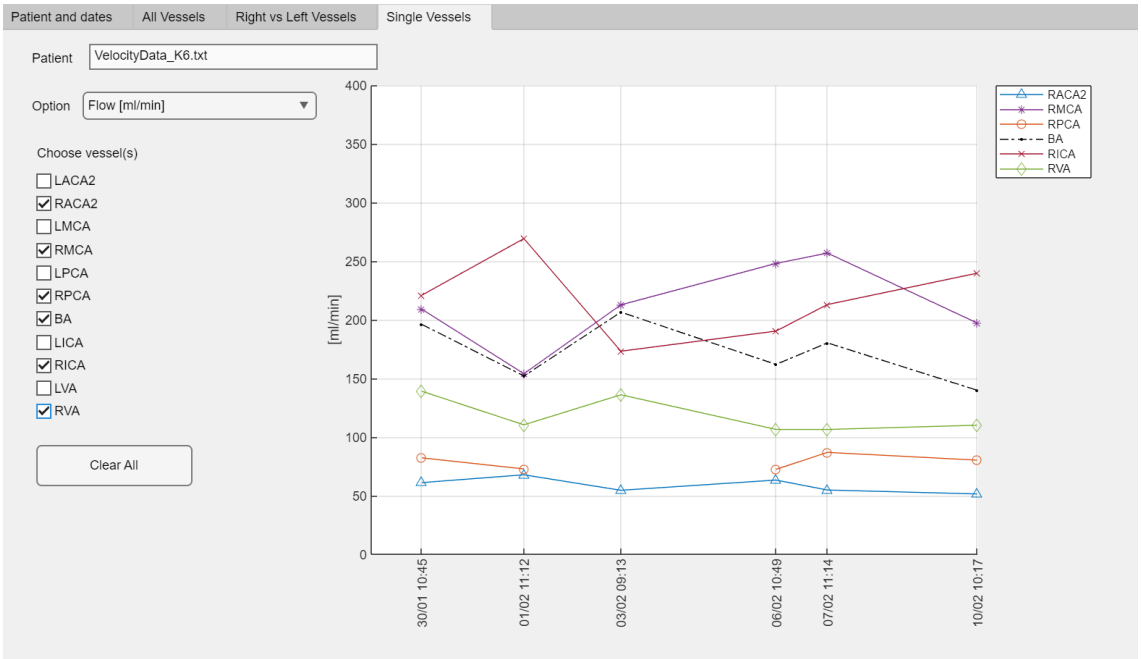

Figure 7.13: Example where multiple vessels have been chosen to be visualized.

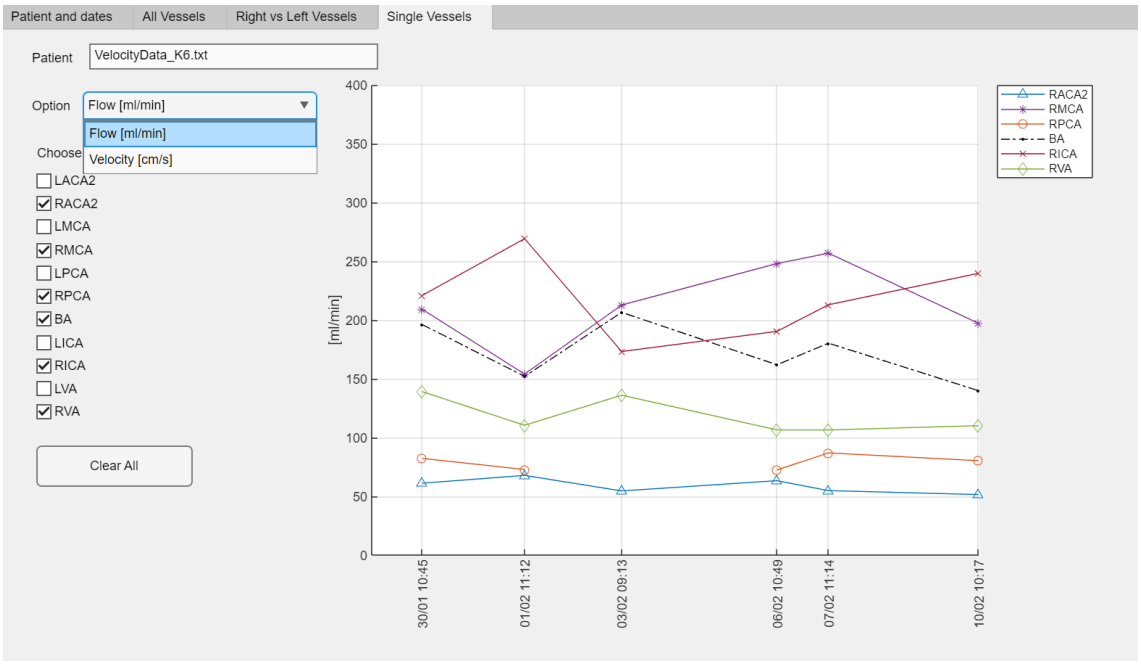

Figure 7.14: Presentation of the dropdown menu and its options for the fourth tab in the GUI

7.8 Limitations

The software requires and assumes that the file with input data contains at least three measurement dates. Limits on the vertical axes of the GUI are set and can thereby not be adapted through the GUI. Colormaps shown in the colorbar in the second tab are also set.